

HR 8844: A NEW TRANSITION OBJECT BETWEEN THE AM STARS AND THE HG MN STARS ?

R. MONIER¹

LESIA, UMR 8109, Observatoire de Paris et Université Pierre et Marie Curie Sorbonne Universités, place J. Janssen, Meudon.

M. GEBRAN²

Department of Physics and Astronomy, Notre Dame University-Louaize, PO Box 72, Zouk Mikael, Lebanon.

F. ROYER³

GEPI, Observatoire de Paris, place J. Janssen, Meudon, France.

T. KILICOGLU⁴

Department of Astronomy and Space Sciences, Faculty of Science, Ankara University, 06100, Turkey.

Y. FRÉMAT⁵

Royal observatory of Belgium, Dept. Astronomy and Astrophysics, Brussels, 8510, Belgium.

ABSTRACT

While monitoring a sample of apparently slowly rotating superficially normal early A stars, we have discovered that HR 8844 (A0 V), is actually a new Chemically Peculiar star. We have first compared the high resolution spectrum of HR 8844 to that of four slow rotators near A0V (ν Cap, ν Cnc, Sirius A and HD 72660) to highlight similarities and differences. The lines of Ti II, Cr II, Sr II and Ba II are conspicuous features in the high resolution high signal-to-noise SOPHIE spectra of HR 8844 and much stronger than in the spectra of the normal star ν Cap. The Hg II line at 3983.93 Å is also present in a 3.5 % blend. Selected unblended lines of 31 chemical elements from He up to Hg have been synthesized using model atmospheres computed with ATLAS9 and the spectrum synthesis code SYNSPEC48 including hyperfine structure of various isotopes when relevant. These synthetic spectra have been adjusted to the mean SOPHIE spectrum of HR 8844, and high resolution spectra of the comparison stars. Chisquares were minimized in order to derive abundances or upper limits to the abundances of these elements for HR 8844 and the comparison stars. HR 8844 is found to have underabundances of He, C, O, Mg, Ca and Sc, mild enhancements of Ti, V, Cr, Mn and distinct enhancements of the heavy elements Sr, Y, Zr, Ba, La, Pr, Sm, Eu and Hg, the overabundances increasing steadily with atomic number. This chemical pattern suggests that HR 8844 may actually be a new transition object between the coolest HgMn stars and the Am stars.

Keywords: stars: early-type – stars: abundances – stars: Chemically Peculiar

1. INTRODUCTION

A bibliographic query of the CDS for HR 8844 actually reveals only 34 publications. HR 8844 appears in Cowley et al.'s classification of the bright A stars and was ascribed an A0V spectral type by these authors. They did not comment on any peculiarity of the spectrum. HR 8844 is also in Eggen's survey of A0 stars (Eggen 1984). It appears as a single star in Eggleton & Tokovinin (2008). The purpose of this paper is to perform a detailed abundance analysis of HR 8844 and show that this star is a new Chemically Peculiar (CP) star.

We have recently undertaken a spectroscopic survey of all apparently slowly rotating bright early A stars (A0-A1V) and late B stars (B8-B9V) observable from the northern hemisphere. This project addresses fundamental questions

of the physics of late-B and early-A stars: i) can we find new instances of rapid rotators seen pole-on (other than Vega) and study their physical properties (gradient of temperature across the disk, limb and gravity darkening), ii) is our census of Chemically Peculiar stars complete up to the magnitude limits we adopted? If not, what are the physical properties of the newly found CP stars? The abundance results for the A0-A1V sample have been published in [Royer et al. \(2014\)](#). Targets have been observed with SOPHIE, the échelle high-resolution spectrograph at Observatoire de Haute Provence yielding spectra covering the 3900–6800 Å spectral range over 39 orders at a resolving power $R = 75000$. A careful abundance analysis of the high resolution high signal-to-noise ratio spectra of the A stars sample and a hierarchical classification have allowed to sort out the sample of 47 A stars into 17 chemically normal stars (ie. whose abundances do not depart by more than ± 0.20 dex from solar values), 12 spectroscopic binaries and 13 Chemically Peculiar stars (CPs) among which five are new CP stars. The status of these new CP stars still needs to be fully specified by spectropolarimetric observations to address their magnetic nature or by exploring new spectral ranges which we had not explored in this first study.

We have now started to examine the B8-B9V sample using the full wavelength coverage provided by SOPHIE to search for new Chemically Peculiar stars. We have already reported on the discovery of 4 new HgMn stars ([Monier et al. 2015](#)) whose spectra display strong Hg II lines at 3984 Å and strong Mn II lines. In the process of our analysis of the B8-B9V sample, we also found that HD 67044 is most likely another new HgMn star ([Monier et al. 2016](#)).

[Royer et al. \(2014\)](#) performed abundance analyses for C, O, Mg, Si, Ca, Sc, Ti, Cr, Fe, Sr, Y, Zr using Takeda’s automated procedure and classified HR 8844 as “probably normal”: the four criteria used for the automatic classification were not fully consistent, depending on the chemical species used. In order to clarify the nature of HR 8844, we have compared its spectra with high resolution high signal-to-noise spectra of 4 stars near A0V and B9V: the superficially normal ν Cap (B9V) and the cool HgMn star ν Cnc, Sirius A (A1m) and HD 72660 (A1m). We have then determined the abundances of 31 chemical elements, in particular helium and several species heavier than barium (not studied in [Royer et al. 2014](#)), for HR 8844 using spectrum synthesis to quantify the enhancements and depletions of these elements or to provide upper limits. We also performed the abundance analysis for the four comparison stars using as much as feasible the same lines and atomic data as employed for HR 8844 for consistency in order to compare the chemical composition of HR 8844 with that of these comparison stars and clarify the nature of this object.

2. OBSERVATIONS AND REDUCTION

We obtained one spectrum of HR 8844 on 05 August 2009 and then secured 3 new spectra in December 2016 at Observatoire de Haute Provence using the high resolution ($R = 75000$) mode of the SOPHIE échelle spectrograph ([Perruchot et al. 2008](#)). The $\frac{\lambda}{\Delta\lambda}$ ratio of the individual spectra ranges from 251 up to 381 at 5500 Å. For ν Cap, we secured four high resolution spectra with HERMES ([Raskin et al. 2011](#)) at the Roque de los Muchachos Observatory. For the three other comparison stars, we fetched spectra from spectroscopic archives. For HD 72660, we fetched a spectrum from the HARPS archive ($R=125000$) and for Sirius A several I profiles obtained with NARVAL from the the Polarbase database ($R=75000$). For ν Cnc, we have retrieved a spectrum from the ELODIE archive ($R=45000$). The observations log of these data for the 5 stars is displayed in Table 1.

The SOPHIE, ELODIE, HARPS, NARVAL and HERMES data are automatically reduced by the individual projects to produce 1D extracted and wavelength calibrated échelle orders. Each reduced order was normalised separately using a Chebychev polynomial fit with sigma clipping, rejecting points above or below 1σ of the local continuum. Normalized orders were then merged together, corrected by the blaze function and resampled into a constant wavelength step of about 0.02 Å (see [Royer et al. 2014](#), for more details). The radial velocity of HR 8844, ν Cap and HD 72660 were derived in [Royer et al. \(2014\)](#) using cross-correlation techniques, avoiding the Balmer lines and the atmospheric telluric lines. The normalized spectrum was cross-correlated with a synthetic template extracted from the POLLUX database¹ ([Palacios et al. 2010](#)) corresponding to the parameters $T_{\text{eff}} = 11000$ K, $\log g = 4$ and solar abundances. A parabolic fit of the upper part of the resulting cross-correlation function yields the Doppler shift, which is then used to shift spectra to rest wavelengths. The projected rotational velocities are taken from [Royer et al. \(2014\)](#) who derived them from the position of the first zero of the Fourier transform of individual lines. The radial velocity and projected equatorial velocity of HR 8844, ν Cap, HD 72660, ν Cap and ν Cnc are collected in Table 2. For Sirius A, they were retrieved from [Landstreet \(2011\)](#).

3. THE LINE SPECTRUM OF HR 8844 - COMPARISON TO ν CAP

¹ <http://pollux.graal.univ-montp2.fr>

Table 1. Observation log for HR 8844, Vega, ν Cap, ν Cnc, Sirius A and HD72660

Star ID	Spectral type	V	Observation Date	Instrument	Resolving power	Exposure time (s)	S/N at 3900 Å	S/N at 5000 Å	S/N at 6000 Å
HR 8844	A0V	5.89	2009-08-05	SOPHIE	75000	600	143	269	274
HR 8844	A0V	5.89	2016-12-12	SOPHIE	75000	900	202	381	389
HR 8844	A0V	5.89	2016-12-13	SOPHIE	75000	400	133	251	256
HR 8844	A0V	5.89	2016-12-14	SOPHIE	75000	600	174	328	335
Vega	A0V	0.00	2012-08-06	SOPHIE	75000	25	309	583	595
ν Cap	B9IV	4.76	2014-08-16	HERMES	85000	150	85	160	163
ν Cap	B9IV	4.76	2014-08-16	HERMES	85000	150	54	102	104
ν Cap	B9IV	4.76	2014-08-16	HERMES	85000	150	87	164	167
ν Cap	B9IV	4.76	2014-08-16	HERMES	85000	150	80	150	153
ν Cnc	B9.5VHgMn	5.45	2005-02-05	ELODIE	42000	3600	182	344	350
Sirius A	A1Vm	-1.46	2007-03-12	NARVAL	75000	2	239	450	459
HD 72660	A0Vm	5.80	2012-02-19	HARPS	125000	117.8	77	146	149

3.1. The line spectrum of HR 8844

In order to establish the chemical peculiarity of HR 8844, we have measured the centroids of all 552 lines absorbing more than 2% of the continuum. Almost all these lines could be identified after we performed a complete synthesis of the spectrum and derived the abundances. The proposed identifications corresponding to the final abundances of HR 8844 are collected in Table 3. The strongest lines (ie. which absorb more than 5% of the continuum) are due to Mg II, Mg I, Ca II (resonance lines), Ca I (idem), Ti II, Cr II, Fe II, Fe I, Sr II and Ba II. Several spectral regions have been inspected to search for the chemical peculiarity of HR 8844. First, the red wing of He ϵ , harbors a line close to the location of the Hg II λ 3983.93 Å line and several Zr II and Y II lines likely to be strengthened in CP stars. After proper correction for the stellar radial velocity, we found that HR 8844 does show a feature next to the Hg II 3983.93 Å line absorbing about 3.5 %, and also the lines of Y II at 3982.59 Å (2 %) and of Zr II at 3991.13 Å (3.5 %) and 3998.97 Å (2 %). Several other lines of Y II and Zr II could be identified in the spectrum of HR 8844 and have been used to derive the abundances of these elements. Second, we examined the region from 4125 Å to 4145 Å for the Si II lines at 4128.054 Å and 4130.894 Å and the Mn II line at 4136.92 Å. This Mn II line is definitely present in HR 8844 but is only a weak line (0.5 %). Similarly, the lines of Mn II at 4206.37 Å and 4252.96 Å absorb respectively 1.5 % and 2.0 %. The abundance analysis of two Mn II lines with hyperfine structure will reveal a manganese excess of about 2 times the solar value.

3.2. Comparison to spectra of ν Cap

HR 8844, Vega and ν Cap have similar effective temperatures, surface gravities and projected equatorial velocities $v_e \sin i$. Differences in the line intensities should therefore reflect mostly differences in chemical compositions. Several spectral regions highlight the differences between HR 8844 and ν Cap. Several lines are stronger in HR 8844 than in ν Cap and Vega which shows that HR 8844 is enriched in the elements responsible for these lines with respect to ν Cap and Vega. We will only show the comparisons with ν Cap here. Figure 1 displays the comparison of the spectra of ν Cap and HR 8844 in the range from 4930 Å to 4940 Å where three lines of C I and the resonance line of Ba II at 4934.096 Å fall. All lines of C I are slightly stronger and the Ba II line is much stronger in HR 8844. Figure 2 displays the comparison of the spectra of ν Cap and HR 8844 in the range 6140 to 6160 Å where several lines of O I fall together with the Fe II lines at 6147.62 Å and 6149.26 Å and the Ba II line at 6141.713 Å. All O I lines are weaker in HR 8844 whereas the Ba II line is much stronger in HR 8844. Figure 3 displays the comparison of the spectra of ν Cap and HR 8844 in the range 4300 to 4320 Å where 4 Ti II lines, the Sc II line at 4314.18 Å and the Sr II line at 4305.443 Å fall. The lines of Ti II, Sc II and Sr II are all stronger in the spectrum of HR 8844 than in that of ν Cap. Figure 4 displays the comparison of the spectra of ν Cap and HR 8844 in the range 4060 Å up to 4080 Å where the Ni II at 4067.04 Å and the Sr II resonance line at 4077.70 Å fall. These two lines are stronger in the spectrum of HR 8844 than in that of ν Cap. Finally, Fig. 5 displays the comparison of the SOPHIE spectra of ν Cap and HR 8844 in the range 4260 up to 4280 Å where the C II doublet at 4267.00 Å and 4267.26 Å and the Cr II lines at 4261.92 Å and 4275.56 Å fall. The C II lines are weaker in HR 8844 than in ν Cap and the Cr II lines are slightly stronger in HR 8844. From these first comparisons, we infer that C, O should be less abundant in HR 8844 than in ν Cap, whereas

Fe may be comparable and Ti, Cr, Ni, Sr and Ba are more abundant in HR 8844 than in ν Cap. Similar trends are found when comparing the spectra of Vega and HR 8844. The abundance analysis carried out in next paragraph will confirm this.

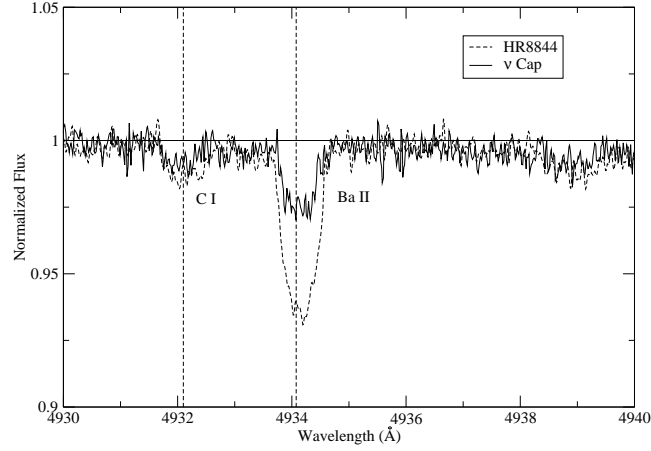


Figure 1. Comparison of the C I lines and the Ba II resonance line at 4934.076 Å in the spectra of ν Cap (solid line) and HR 8844 (dashed lines)

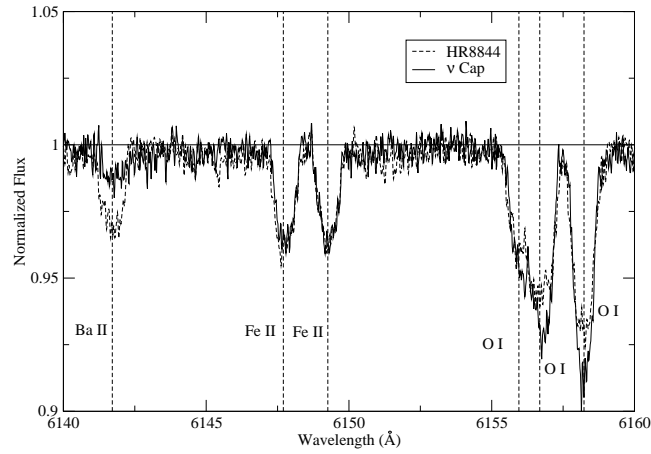


Figure 2. Comparison of the O I lines at 6155.87, 6156.62 and 6158.17 Å, the Ba II line at 6141.713 Å in the spectra of ν Cap (solid line) and HR 8844 (dashed lines)

4. ABUNDANCE DETERMINATIONS FOR HR 8844, ν CAP, ν CNC, SIRIUS A AND HD 72660

4.1. Fundamental parameters determinations

For HR 8844, ν Cap and ν Cnc, we have applied Napiwotzky's (1993) UVBYBETA procedure to derive the effective temperature and surface gravity. The fundamental parameters of Sirius A and HD 72660 were taken respectively from Landstreet (2011) and Golriz & Landstreet (2016). The adopted effective temperatures, surface gravities, projected equatorial velocities and radial velocities for HR 8844, Vega, ν Cap, ν Cnc, Sirius A and HD 72660 are collected in Table 2. The adopted values for the parameters of HR8844 are in good agreement with the spectroscopic determination of Gebran et al. (2016). The projected equatorial velocities and radial velocities of HR 8844 and HD 72660 are taken from Royer et al. (2014) and for ν Cap from Royer et al. (2002).

4.2. Microturbulent velocity determination

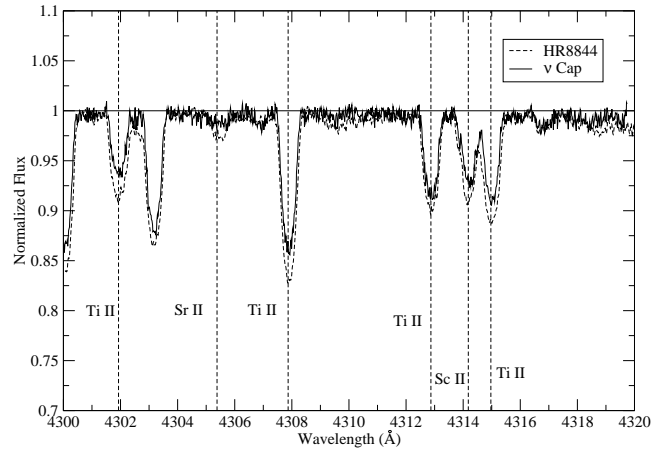


Figure 3. Comparison of four Ti II lines, the Sr II line at 4305.443 Å and the Sc II line at 4314.18 Å in the spectra of ν Cap (solid line) and HR 8844 (dashed lines)

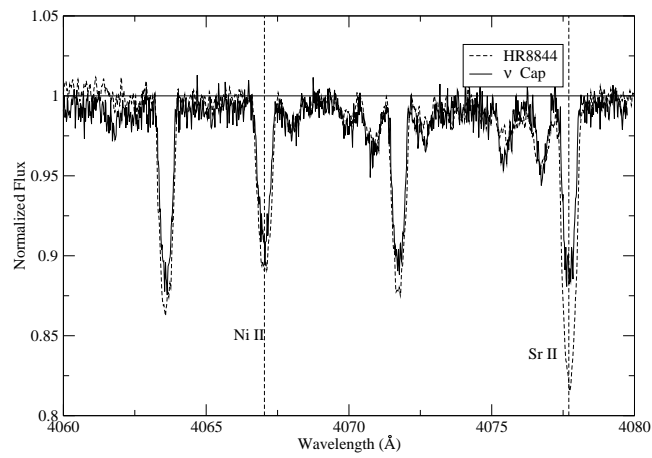


Figure 4. Comparison of the Ni II lines at 4067.04 Å, the Sr II resonance line at 4077.70 Å in the spectra of ν Cap (solid line) and HR 8844 (dashed lines)

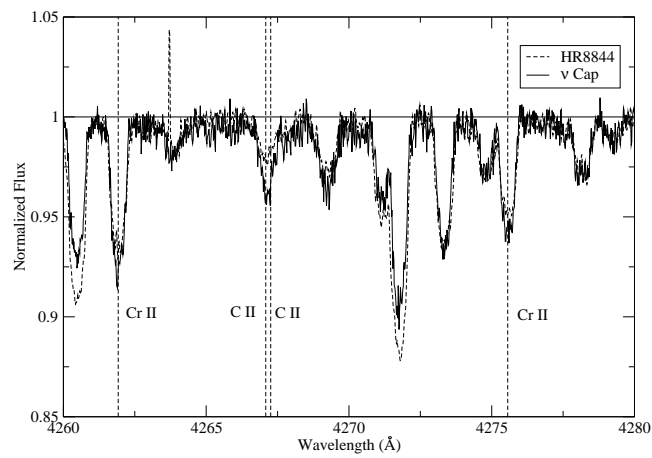
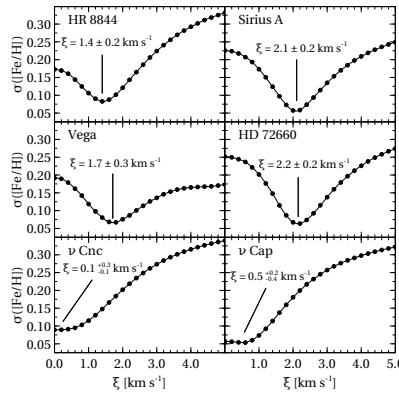


Figure 5. Comparison of the C II doublet at 4267.00 and 4267.26 Å and the Cr II lines at 4261.92 and 4275.56 Å in the spectra of ν Cap (solid line) and HR 8844 (dashed lines)

Table 2. Adopted fundamental parameters for HR 8844, Vega, ν Cap, ν Cnc, Sirius A, HD 72660

Star ID	T_{eff} (K)	$\log g$	$v \sin i$ (km s^{-1})	V_{rad} (km s^{-1})	ξ (km s^{-1})
HR 8844	9752 ± 250	3.80 ± 0.25	27.3 ± 0.3	-4.48 ± 0.21	1.40 ± 0.20
Vega	9500 ± 250	4.00 ± 0.25	27.0 ± 0.3	-17.51 ± 0.02	1.70 ± 0.30
ν Cap	10300 ± 250	3.90 ± 0.25	24.0 ± 0.3	-11.39 ± 0.20	0.50 ± 0.20
ν Cnc	10300 ± 250	3.67 ± 0.25	18.0 ± 0.3	-20.04 ± 0.20	0.10 ± 0.20
Sirius A	9900 ± 250	4.30 ± 0.25	16.5 ± 0.3	variable	2.10 ± 0.30
HD 72660	9650 ± 250	4.05 ± 0.25	5.0 ± 0.5	4.50 ± 0.07	2.20 ± 0.20

In order to derive the microturbulent velocity of HR 8844, Vega, ν Cap, ν Cnc, Sirius A and HD 72660, we have simultaneously derived the iron abundance $[\text{Fe}/\text{H}]$ for 50 unblended Fe II lines and a set of microturbulent velocities ranging from 0.0 to 5.0 km s^{-1} . Figure 6 shows the standard deviation of the derived $[\text{Fe}/\text{H}]$ as a function of the microturbulent velocity. The adopted microturbulent velocities are the values which minimize the standard deviations ie. for that value, all Fe II lines yield the same iron abundance. We therefore adopt a microturbulent velocity $\xi_t = 1.4 \pm 0.2 \text{ km s}^{-1}$ constant with depth for HR 8844. The microturbulent velocities of the six stars are collected in Table 2.

**Figure 6.** Determination of the microturbulent velocities of HR 8844, Vega, ν Cap, ν Cnc, Sirius A and HD 72660.

4.3. Model atmospheres and spectrum synthesis calculations

Plane parallel model atmospheres assuming radiative equilibrium and hydrostatic equilibrium were computed using the ATLAS9 code (Kurucz 1992) for the appropriate fundamental parameters of each star. The linelist was built from Kurucz’s gfall21oct16.dat² which includes hyperfine splitting levels. The observed wavelengths and oscillator strengths were retrieved by querying the NIST³. For the other species which lack data in the Atomic Spectra Database, we have used other references to retrieve their atomic data which are collected in Tab. 5. A grid of synthetic spectra was computed with SYNSPEC48 (Hubeny & Lanz 1992) to model the lines of 31 elements for HR8844 and ν Cap. Computations were iterated varying the unknown abundance until minimization of the chi-square between the observed and synthetic spectrum was achieved. Abundances are derived for 34 elements for ν Cnc, 37 elements for Sirius A and 37 elements for HD 72660 because these three stars have significantly lower projected rotational velocities.

4.4. The derived abundances of HR 8844

We have used only unblended lines to derive the abundances. For a given element, the final abundance is a weighted mean of the abundances derived for each transition (the weights are derived from the NIST grade assigned to that

² <http://kurucz.harvard.edu/linelists/gfnew/gfall21oct16.dat>

³ <http://www.nist.gov/> Atomic Spectra Database (Kramida et al. 2017) for the following atoms or ions: He I, C II, O I, Mg II, Al I, Al II, Si II, S II, Ca II, Sc II, Ti II, Cr II, Mn II, Fe II, Sr II, Ba II and Dy II

particular transition). For several elements, in particular the heaviest elements, only one unblended line was available. These final abundances and their estimated uncertainties for HR 8844 are collected in Tab. 4. The determination of the uncertainties is discussed in the Appendix. Table 4 contains for each analysed species the adopted laboratory wavelength, logarithm of oscillator strength, its source, the logarithm of the absolute abundance normalised to that of hydrogen (on a scale where $\log(N_H) = 12$) for each transition, and the solar abundance adopted for that element. In this work, we adopted [Grevesse & Sauval \(1998\)](#) abundances for the Sun as a reference. The final mean abundance and its estimated uncertainty are then given.

The light elements, He, C, O, Mg are found to be depleted in HR 8844. The helium abundance is found to be about 0.70 times the solar abundance of helium consistently from the He I lines near 4471 Å and near 5875.5 Å. The NLTE abundance correction for the λ 4471.48 Å He I line is very small as shown by [Lemke \(1989\)](#) for early A-type stars and we have not corrected for it. Carbon is depleted, about 0.40 times the solar abundance from the analysis of the C II triplet at 4267 Å. Oxygen is depleted about 0.80 times the solar oxygen abundance from 12 O I transitions near 5330 Å and from 6155 to 6158 Å. Magnesium is also depleted by 0.45 times the solar abundance, aluminium is 0.8 times solar and silicon is about solar. Calcium and scandium are depleted by 0.70 times the solar abundances. As from titanium, all elements start to be mildly overabundant, except for iron. From the analysis of 12 lines, titanium is found to be about 1.41 times enriched respect to the solar abundance. The vanadium abundance is 1.88 times the solar abundance and the chromium abundance 1.45 times the solar abundance. The Mn II lines at 4206.37 Å and 4259.19 Å include hyperfine structure of the isotopes of manganese and yield 2 times the solar manganese abundance. The iron abundance which is solar has been derived mostly by using 16 Fe II lines of multiplets 37, 38 and 186 in the range 4500–4600 Å whose atomic parameters are critically assessed in NIST (these are C+ and D quality lines). These lines are widely spaced and the continuum is fairly easy to trace in this spectral region. Their synthesis always yields consistent iron abundances from the various transitions with very little dispersion. The iron abundance is probably the most accurately determined of the abundances derived here. The Sr-Y-Zr triad is overabundant by modest amounts: about 5 times solar for strontium, about 5 times for yttrium and 5.8 times solar for zirconium. Barium is enhanced by a factor of 9.3 and the Lanthanides by factors of 15 up to 100 times solar. Figure 7 illustrates the detection of a 10 times solar overabundance for barium from the Ba II line at 4554.03 Å.

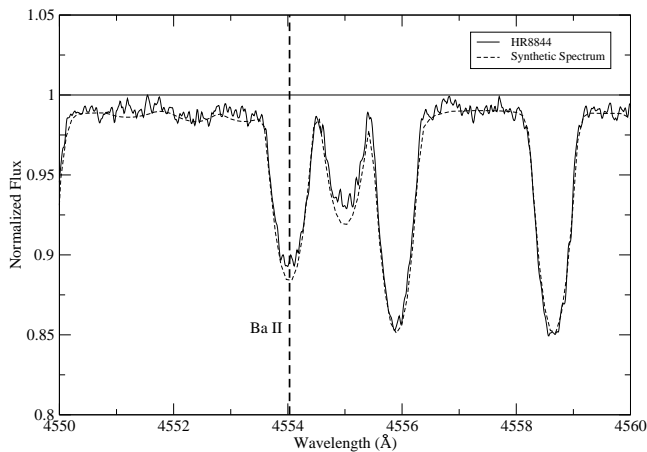


Figure 7. Determination of the barium overabundance from the Ba II line at 4554.03 Å in HR 8844

Mercury is enhanced by 10000 times the solar value. The overall abundance pattern of HR 8844 is therefore that light species tend to be almost all underabundant (He, C, O, Mg, Si, Ca, Sc) while the iron-peak elements show mild enhancements (less than 5 times solar) and Sr, Y, Zr, Ba, the Lanthanides and Hg show more and more pronounced overabundances (larger than 5 times solar), the largest overabundance being for Hg. The general trend therefore is that the heaviest elements are the most overabundant which strongly suggests that atomic diffusion be responsible for the chemical pattern of HR 8844.

The derived abundances of HR 8844 are compared to the previous determination in [Royer et al. \(2014\)](#) for the twelve elements in common in Tab. 7 and figure 8. We find a reasonably good agreement (within ± 0.25 dex) for C, O, Ca, Sc, Cr, Fe and Sr.

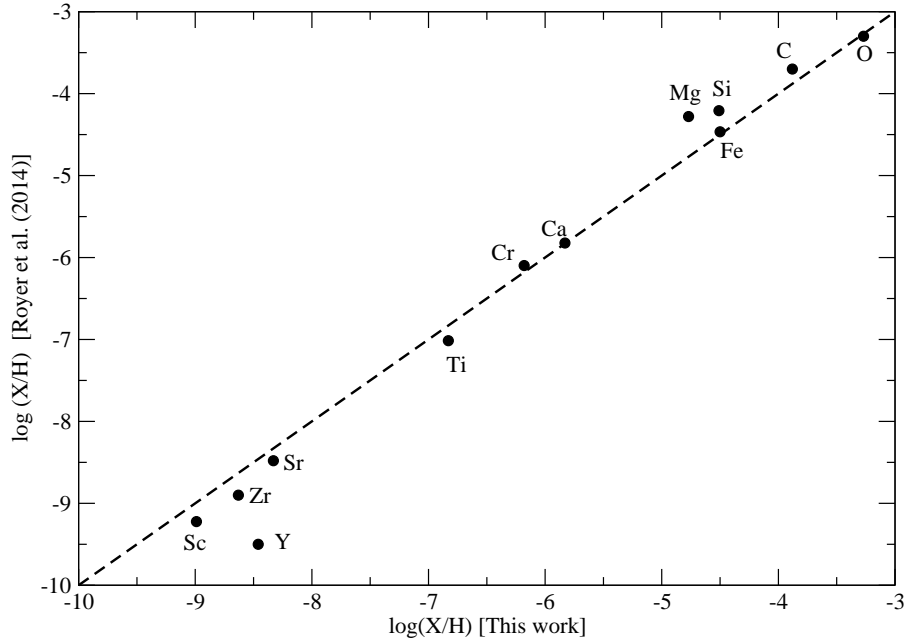


Figure 8. Comparison of the abundances derived in Royer et al. (2014) and this work for the twelve elements in common

4.5. The derived abundances for the comparison stars ν Cap, ν Cnc, Sirius A and HD 72660

Using the same method and linelist, we have derived the elemental abundances of the normal star ν Cap, the cool HgMn star ν Cnc and the hot Am stars Sirius A and HD 72660 in order to compare the found abundances of HR 8844 to those of these four stars. The found abundances for these four comparison stars are collected in Tab. 5.

We have compared the derived abundances for these four stars with published abundance studies in the literature as displayed in Tab. 7. We expect differences with previous analyses because of i) differences in the adopted $v_e \sin i$ or ξ and ii) differences in the lines used and their atomic data. The found abundances for ν Cap are very close to solar for most elements in agreement with Adelman (1991) and Smith & Dworetzky (1993). This star proves to be a very good normal comparison star. The abundances in Adelman (1991) differ slightly from ours for three reasons. Although he did use a similar effective temperature and surface gravity, Adelman adopted a null microturbulent velocity for ν Cap whereas we use 0.50 km s^{-1} . We did not necessarily use the same lines for a given element and the atomic data for the few lines have been upgraded to the latest values compiled in NIST.

For ν Cnc, our abundances are almost all larger than those reported in Adelman (1989). He did use fundamental parameters and a microturbulent velocity similar to ours, however he adopted a smaller $v_e \sin i = 13 \text{ km s}^{-1}$ whereas we use 18 km s^{-1} . We therefore have to slightly enhance the abundances to reproduce the observed profiles. Note that we determine here for the first time the abundances of several Lanthanides in ν Cnc.

For Sirius A, we have compared our results with the most recent determinations of Landstreet (2011) for the elements up to Nickel and Cowley et al. (2016) for heavier elements. We use the same effective temperature, surface gravity and a slightly lower microturbulent velocity (2.10 km s^{-1} rather than 2.20 km s^{-1} adopted by these authors). In his paper, Landstreet (2011) emphasizes that even for Sirius large differences in elemental abundances remain for C, Mg, Al, Si, S, Ca, V, Mn, Ni and even Fe from one author to another. We find good agreement (ie. within ± 0.20 dex) with Landstreet’s (2011) abundances for O, Ca, Cr, Mn, Fe, Ni, Sr, Ba. For elements heavier than barium, we find a fair agreement with Cowley et al. (2016) abundances for La, Pr, Nd, Sm and Hf within ± 0.20 dex of their determinations. For HD 72660, we have compared our abundances with those of Golriz & Landstreet (2016) as we have used similar effective temperature, surface gravity, projected equatorial velocity and microturbulent velocity. We find a fair agreement with Golriz & Landstreet (2016) for the abundances of several elements: C, Mg, Al, Si, S, Sc, Ti, V, Cr, Ni and Zr.

In Fig. 9, we compare the found abundances for HR 8844 with our new determinations for the four comparison stars.

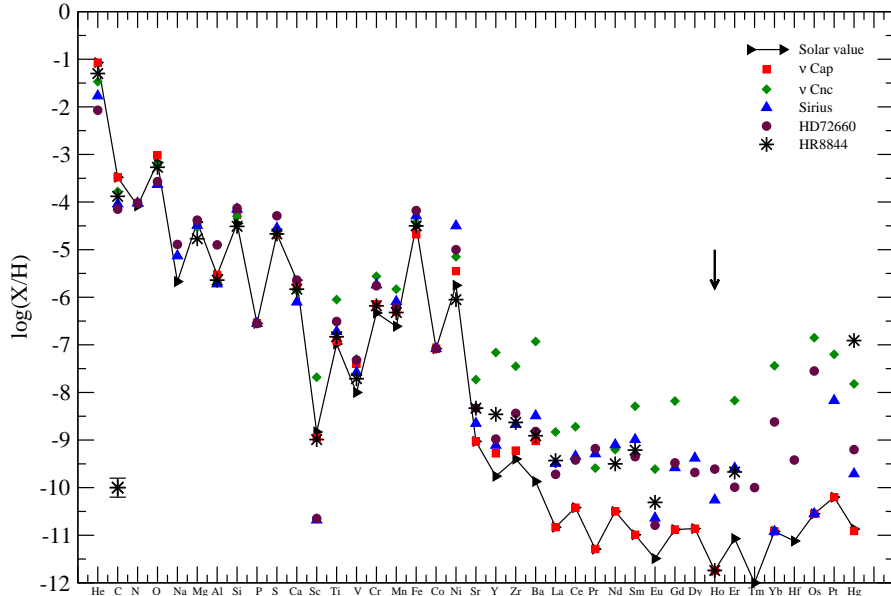


Figure 9. Comparison of the abundance pattern of HR 8844, to those of ν Cap, ν Cnc, Sirius A and HD 72660.

As ν Cnc, and Sirius A, HR 8844 displays the characteristic underabundances for most elements lighter than titanium and pronounced overabundances for elements heavier which Chemically Peculiar stars harbour. The overabundances of HR 8844 are modest for the iron-peak elements but increase for the Sr-Y-Zr triad and barium (of the order of 10 times solar) and for the Lanthanides and of the order of 10^2 solar for mercury. The overabundance of manganese and mercury, the underabundances of calcium and scandium and of the lightest elements, the mild overabundances of the iron-peak elements, of the Sr-Y-Zr triad, of barium and several Rare Earths show that HR 8844 is a new hot Am star which also displays characteristic enhancements of the coolest HgMn stars (as HD 72660 and Sirius A do). We therefore propose that HR 8844 be a new transition object between the Am stars and the coolest HgMn stars and as such is a very interesting star.

5. CONCLUSION

We report here on detailed abundance determinations of the A0V star HR 8844, hitherto considered as a "normal star". Our analysis definitely establishes that HR 8844 is a new Chemically Peculiar star, probably a hot Am star (as Sirius A and HD 72660 are) extending the realm of Am stars to significantly higher temperatures. As HD 72660 and Sirius A, HR 8844 may well be a transition object between the Am stars and the coolest HgMn star and as such is a very interesting object. We are undertaking a monitoring of HR 8844 over its rotation period (which must be smaller than 5 days assuming a radius of about 2 solar radii for an A0V star) to search for variability due to the presence of spots or a companion.

APPENDIX

A. DETERMINATION OF UNCERTAINTIES

For a representative line of a given element, six major sources are included in the uncertainty determinations: the uncertainty on the effective temperature ($\sigma_{T_{\text{eff}}}$), on the surface gravity ($\sigma_{\log g}$), on the microturbulent velocity (σ_{ξ_t}), on the apparent rotational velocity ($\sigma_{v_e \sin i}$), the oscillator strength ($\sigma_{\log gf}$) and the continuum placement (σ_{cont}). These uncertainties are supposed to be independent, so that the total uncertainty σ_{tot_i} for a given transition (i) is:

$$\sigma_{\text{tot}_i}^2 = \sigma_{T_{\text{eff}}}^2 + \sigma_{\log g}^2 + \sigma_{\xi_t}^2 + \sigma_{v_e \sin i}^2 + \sigma_{\log gf}^2 + \sigma_{\text{cont}}^2. \quad (\text{A1})$$

The mean abundance $\langle [\frac{X}{H}] \rangle$ is then computed as a weighted mean of the individual abundances $[X/H]_i$ derived for each transition (i):

$$\langle [\frac{X}{H}] \rangle = \frac{\sum_i ([\frac{X}{H}]_i / \sigma_{\text{tot}_i}^2)}{\sum_i (1 / \sigma_{\text{tot}_i}^2)} \quad (\text{A2})$$

and the total error, σ is given by:

$$\frac{1}{\sigma^2} = \sum_{i=1}^N (1/\sigma_{tot_i}^2) \quad (\text{A.3})$$

where N is the number of lines per element. The uncertainties σ for each element are collected in Tab. 4.

RM thanks Pr. Charles Cowley and Pr. David Gray for their insightful comments during the analysis of HR 8844. We thank the OHP night assistants for their helpful support during the three observing runs. This work has made use of the VALD database (Ryabchikova et al. 2011), operated at Uppsala University, the Institute of Astronomy RAS in Moscow, and the University of Vienna. We have also used the NIST Atomic Spectra Database (version 5.4) available <http://physics.nist.gov/asd>. We also acknowledge the use of the ELODIE archive at OHP available at <http://atlas.obs-hp.fr/elodie/>.

REFERENCES

- Adelman, S. J. 1989, MNRAS, 239, 487
 Adelman, S. J. 1991, MNRAS, 252, 116
 Biéumont, É., Blagoev, K., Engström, L., et al. 2011, MNRAS, 414, 3350
 Biéumont, E., Grevesse, N., Faires, L. M., Marsden, G., & Lawler, J. E. 1989, A&A, 209, 391, (BGF)
 Butler, K. & Zeippen, C. J. 1991, J. Phys. IV France, 01, C1
 Cowley, A., Cowley, C., Jaschek, M., & Jaschek, C. 1969, AJ, 74, 375
 Cowley, C. R., Ayres, T. R., Castelli, F., et al. 2016, ApJ, 826, 158
 Davidson, M. D., Snoek, L. C., Volten, H., & Doenszelmann, A. 1992, A&A, 255, 457
 Den Hartog, E. A., Lawler, J. E., Sneden, C., & Cowan, J. J. 2006, ApJS, 167, 292
 Dolk, L., Wahlgren, G. M., & Hubrig, S. 2003, A&A, 402, 299
 Drake, G. 2006, Springer Handbook of Atomic, Molecular, and Optical Physics, ed. G. Drake (New York, NY: Springer New York), 199–219
 Eggen, O. J. 1984, ApJS, 55, 597
 Eggleton, P. P. & Tokovinin, A. A. 2008, MNRAS, 389, 869
 Gebran, M., Farah, W., Paletou, F., Monier, R., & Watson, V. 2016, A&A, 589, A83
 Golriz, S. S. & Landstreet, J. D. 2016, MNRAS, 456, 3318
 Grevesse, N. & Sauval, A. J. 1998, SSRv, 85, 161
 Hubeny, I. & Lanz, T. 1992, A&A, 262, 501
 Kling, R., Schnabel, R., & Griesmann, U. 2001, The Astrophysical Journal Supplement Series, 134, 173
 Kramida, A., Ralchenko, Y., Reader, J., & NIST ASD Team. 2017, <http://physics.nist.gov/asd>, 5
 Kurucz, R. L. 1992, RMxAA, 23
 Kurucz, R. L. 1993, (GUES)
 Kurucz, R. L. 2003, Robert L. Kurucz on-line database of observed and predicted atomic transitions
 Kurucz, R. L. 2010, Robert L. Kurucz on-line database of observed and predicted atomic transitions
 Kurucz, R. L. & Peytremann, E. 1975, SAO Special Report, 362, 1, (KP)
 Landstreet, J. D. 2011, A&A, 528, A132
 Lawler, J. E., Den Hartog, E. A., Sneden, C., & Cowan, J. J. 2006, ApJS, 162, 227
 Lawler, J. E., Sneden, C., & Cowan, J. J. 2004, ApJ, 604, 850
 Lawler, J. E., Sneden, C., Cowan, J. J., Ivans, I. I., & Den Hartog, E. A. 2009, Astrophys. J. Suppl. Ser., 182, 51, (LSCI)
 Lawler, J. E., Sneden, C., Cowan, J. J., et al. 2008, ApJS, 178, 71
 Lawler, J. E., Wickliffe, M. E., Cowley, C. R., & Sneden, C. 2001a, ApJS, 137, 341
 Lawler, J. E., Wickliffe, M. E., den Hartog, E. A., & Sneden, C. 2001b, Astrophys. J., 563, 1075, (LWHS)
 Lemke, M. 1989, A&A, 225, 125
 Ljung, G., Nilsson, H., Asplund, M., & Johansson, S. 2006, A&A, 456, 1181
 Martin, W. C. 1960, J. Opt. Soc. Am., 50, 174
 Meggers, W. F., Corliss, C. H., & Scribner, B. F. 1975a, Tables of spectral-line intensities. Part I, II_- arranged by elements.
 Meggers, W. F., Corliss, C. H., & Scribner, B. F. 1975b, Tables of spectral-line intensities. Part I, II_- arranged by elements., ed. Meggers, W. F., Corliss, C. H., & Scribner, B. F., (MC)
 Miles, B. M. & Wiese, W. L. 1969, Atomic Data, 1, 1
 Miller, M. H., Wilkerson, T. D., Roig, R. A., & Bengtson, R. D. 1974, PhRvA, 9, 2312, (MWRB)
 Monier, R., Gebran, M., & Royer, F. 2015, A&A, 577, A96
 Monier, R., Gebran, M., & Royer, F. 2016, Ap&SS, 361, 139
 Napiwotzki, R., Schoenberner, D., & Wenske, V. 1993, A&A, 268, 653
 Palacios, A., Gebran, M., Josselin, E., et al. 2010, A&A, 516, A13
 Palmeri, P., Quinet, P., Wyart, J., & Biéumont, E. 2000, Physica Scripta, 61, 323, (PQWB)
 Perruchot, S., Kohler, D., Bouchy, F., et al. 2008, in Proc. SPIE, Vol. 7014, Ground-based and Airborne Instrumentation for Astronomy II, 70140J
 Pinnington, E. H., Berends, R. W., & Lumsden, M. 1995, Journal of Physics B: Atomic, Molecular and Optical Physics, 28, 2095
 Raassen, A. J. J. & Uylings, P. H. M. 1998, Journal of Physics B Atomic Molecular Physics, 31, 3137
 Raskin, G., van Winkel, H., Hensberge, H., et al. 2011, A&A, 526, A69
 Royer, F., Gebran, M., Monier, R., et al. 2014, A&A, 562, A84
 Royer, F., Grenier, S., Baylac, M.-O., Gómez, A. E., & Zorec, J. 2002, A&A, 393, 897
 Ryabchikova, T., Ryabtsev, A., Kochukhov, O., & Bagnulo, S. 2006, Astron. and Astrophys., 456, 329, (RRKB)
 Ryabchikova, T. A., Pakhomov, Y. V., & Piskunov, N. E. 2011, Kazan Izdatel Kazanskogo Universiteta, 153, 61
 Ryabtsev, A. N. 2010, private communication, (ISAN)
 Sansonetti, C. J. & Nave, G. 2014, The Astrophysical Journal Supplement Series, 213, 28
 Sansonetti, C. J. & Reader, J. 2001, Physica Scripta, 63, 219
 Shenstone, A. G. 1961, Proceedings of the Royal Society of London A: Mathematical, Physical and Engineering Sciences, 261, 153

- Smith, K. C. & Dworetsky, M. M. 1993, *A&A*, 274, 335
- Theodosiou, C. E. 1989, *PhRvA*, 39, 4880
- Wickliffe, M. E., Lawler, J. E., & Nave, G. 2000, *J. Quant. Spectrosc. Radiat. Transfer*, 66, 363, (WLN)
- Wiese, W. L., Fuhr, J. R., & Deters, T. M. 1996, *Atomic transition probabilities of carbon, nitrogen, and oxygen : a critical data compilation*
- Wood, M. P., Lawler, J. E., Den Hartog, E. A., Sneden, C., & Cowan, J. J. 2014, *ApJS*, 214, 18
- Zhiguo, Z., Li, Z. S., Lundberg, H., et al. 2000, *Journal of Physics B Atomic Molecular Physics*, 33, 521, (ZLLZ)
- Zhiguo, Z., Zhongshan, L., & Zhankui, J. 1999, *The European Physical Journal D - Atomic, Molecular, Optical and Plasma Physics*, 7, 499

Table 1. Line identifications for HR 8844

λ_{obs} (Å)	λ_{lab} (Å)	Identification	$\log gf$	E_{low}	Comments
3900.55	3900.515	Fe I	-0.92	26140.176	
3900.55	3900.550	Ti II	-0.45	9118.260	
3903.08	3902.945	Fe I	-0.47	12560.933	
3903.99	3903.99	Fe I	-2.53	34121.602	
3905.58	3905.525	Si I	-1.09	15394.369	
3905.78	3905.644	Cr II	-0.90	42986.619	
3906.18	3906.035	Fe II	-1.83	44929.549	
3920.44	3920.26	Fe I	-1.75	978.074	
3922.93	3922.912	Fe I	-1.65	415.933	
3927.98	3927.92	Fe I	-1.59	888.132	
	3927.925	Fe I	-2.19	22838.320	
3930.28	3930.296	Fe I	-1.590	704.007	
	3930.304	Fe II	-4.030	13671.086	
3932.99	3932.023	Ti II	-1.780	9118.260	
3933.65	3933.660	Ca II	0.130	0.000	no IS comp.
3935.88	3935.813	Fe I	-0.770	22838.320	
3938.29	3938.289	Fe II	-3.890	13474.411	
3938.45	3938.400	Mg I	-0.760	35051.263	
3943.97	3944.006	Al I	-0.620	0.000	
3944.01	3944.101	Ni I	+0.130	29320.783	
3945.32	3945.210	Fe II	-4.250	13673.186	
3946.51	3946.487	Ni II	-1.600	76402.031	
3947.42	3947.480	O I	-2.430	73768.202	
3948.99	3949.056	La II	0.410	3250.350	?
3949.85	3949.953	Fe I	-1.160	17550.800	
3950.28	3950.352	Y II	-0.490	840.213	
	3950.389	Dy II	0.100	10953.940	
3951.14	3951.150	Fe I	-0.600	33412.716	
	3951.163	Fe I	-0.380	26406.404	
3952.06	3951.065	V II	-0.740	11908.270	
3956.71	3956.710	Fe I	-0.430	21715.731	

Table 1 continued on next page

Table 1 (*continued*)

λ_{obs} (Å)	λ_{lab} (Å)	Identification	$\log gf$	E_{low}	Comments
3961.60	3961.600	Al I	-0.320	112.061	
3968.50	3968.469	Ca II	-0.170	0.000	
3979.59	3979.505	Cr II	-0.730	45730.581	
3981.81	3981.771	Fe I	-1.080	21999.128	
3983.951	3983.838	Hg II	-3.000	35514.000	hfs iso
3983.957	3983.844	Hg II	-3.130	35514.000	
3983.966	3983.853	Hg II	-3.000	35514.000	
3984.025	3983.912	Hg II	-2.500	35514.000	
3984.045	3983.932	Hg II	-3.100	35514.000	
3984.054	3983.941	Hg II	-2.900	35514.000	
3984.106	3983.993	Hg II	-2.400	35514.000	
3984.185	3984.072	Hg II	-1.700	35514.000	
3984.12	3984.183	Mn I	-1.490	25280.982	
3986.57	3986.581	Mn II	-2.600	44138.961	
3987.84	3987.930	Fe I	-1.800	33412.716	
3991.01	3990.977	Fe II	-1.600	79331.503	
3994.03	3994.006	Fe II	-1.810	88723.398	
3997.31	3997.392	Fe I	-0.390	21999.129	
3998.88	3998.985	Zr II	-0.520	4205.500	
4002.14	4002.083	Fe II	-3.470	22409.852	
4002.67	4002.592	Si II	-0.610	83801.952	
4003.08	4003.146	Mn II	-9.831	109241.500	
4003.59	?				
4005.17	4005.242	Fe I	-0.640	12560.933	
4005.44	4005.467	Tb II	0.570	1016.380	
4005.70	4005.706	V II	-0.460	14655.630	
4005.86	4005.804	Mn II	-1.350	81993.850	
4009.73	4009.713	Fe I	-1.200	17927.381	blend
4012.31	4012.385	Ti II	-1.610	4628.580	
	4012.386	Ce II	0.470	4523.033	
4012.42	4012.386	Ce II	0.470	4253.033	
4012.50	4012.496	Cr II	-0.890	45669.369	

Table 1 continued on next page

Table 1 (*continued*)

λ_{obs} (Å)	λ_{lab} (Å)	Identification	$\log gf$	E_{low}	Comments
4012.59	?				
4014.56	4014.531	Fe I	-0.200	24574.652	
4015.58	4015.506	Fe I	-0.950	33695.394	
4017.30	4017.282	V II	-1.210	30613.920	
4021.68	4021.728	Nd II	-0.300	1470.105	
4021.88	4021.866	Fe I	-0.660	22249.428	
4023.20	4023.220	Sm II	-1.070	326.460	
4023.51	4023.520	Ca I	-2.270	23652.305	
	4023.578	La II	-0.600	14375.170	
4024.53	4024.547	Fe II	-2.480	36252.917	
4024.66	4024.725	Fe I	-0.710	26140.178	
4025.24	4025.223	C I	-2.870	60362.630	
4026.29	4026.187	He I	-0.700	169086.867	
	4026.318	Al II	-1.740	110089.834	
4028.22	4028.322	Dy II	1.27	20884.419	
4028.39	4028.338	Ti II	-0.960	15257.553	
	4028.465	Si II	-0.360	84004.259	
4029.56	4029.622	Fe I	-1.940	26339.695	
4029.88	4029.684	Zr II	-0.600	5752.920	
4030.58	4030.488	Fe I	-0.550	25893.936	
4033.020	4032.940	Fe II	-2.570	36254.622	
	4033.070	Mn I	-0.620	0.000	
4035.59	4035.595	Fe I	-1.100	34039.315	5 % line
	4035.604	V II	-0.960	4035.604	
4036.80	4036.806	Cr I		20520.900	
4037.98	4037.972	Cr II	-0.560	52321.010	
4041.39	4041.360	Mn I	0.280	17052.289	
4043.97	4043.897	Fe I	-0.830	26140.178	broad blend
	4043.977	Fe I	-1.130	26140.178	
	4044.012	Fe I	-2.410	44929.438	
4045.81	4045.812	Fe I	+0.280	11976.238	18 % line
4048.83	4048.831	Fe II	-2.150	44917.017	asymmetric

Table 1 continued on next page

Table 1 (*continued*)

λ_{obs} (Å)	λ_{lab} (Å)	Identification	$\log gf$	E_{low}	Comments
4051.87	4051.930	Cr II	-2.190	25033.700	
4053.85	4053.834	Ti II	-1.210	15265.119	
4057.46	4057.461	Fe II	-1.550	58668.776	
	4057.442	Dy II	0.960	23707.180	
	4057.505	Mg I	-1.200	35031.263	
4063.58	4063.594	Fe I	0.07	12560.933	14 % blend
4063.69	4063.637	Fe I	-0.800	33095.940	idem
4063.70	4063.733	Mn I	-1.760	34250.619	idem
	4063.848	Mn I	-0.650	37789.930	idem
4067..04	4067.031	Ni II	-1.830	32496.075	
4068.04	4067.978	Fe I	-0.130	25899.986	
4070.86	4070.840	Cr II	-0.750	52321.189	
4071.73	4071.738	Fe I	-0.020	12968.554	
	4071.775	Ce II	-0.150	2634.686	12 % line
4075.58	4075.623	Cr II	-3.470	25035.399	
4076.75	4076.780	Si II	-1.700	79338.502	broad blend
	4076.800	Fe I	-1.180	26339.695	
4077.73	4077.709	Sr II	0.170	0.000	
4118.57	4118.545	Fe I	0.280	28819.950	broad blend
4122.72	4122.638	Fe II	-3.300	20830.553	
4128.02	4128.054	Si II	0.360	79338.502	
4128.84	4128.735	Fe II	-3.600	20830.553	
4130.88	4130.872	Si II	-0.780	79355.019	
	4130.890	Si II	0.550	79355.019	
4132.14	4132.058	Fe I	-0.650	12968.554	
4134.71	4134.677	Fe I	-0.490	22838.320	
4136.97	4136.902	Mn II	-1.250	49514.374	
	4136.998	Fe I	-0.540	27543.002	
4143.39	4143.415	Fe I	-0.200	24574.652	
	4143.430	N I	-2.090	83317.831	
4143.73	4143.826	Fe I	-1.270	23051.748	
	4143.868	Fe I	-0.450	12560.934	

Table 1 continued on next page

Table 1 (*continued*)

λ_{obs} (Å)	λ_{lab} (Å)	Identification	$\log gf$	E_{low}	Comments
4144.02	4144.078	Fe I	-2.565	58906.436	
4145.78	4145.782	Cr II	-1.160	42900.629	
4149.23	4149.217	Zr II	-0.030	6467.610	
4154.67	4154.499	Fe I	-0.690	22838.320	
	4154.805	Fe I	-0.370	27166.817	
4161.522	4161.535	Ti II	-2.360	8744.250	
4162.73	4162.665	S II	0.780	128599.162	
4163.59	4163.644	Ti II	-0.130	20891.790	
4167.28	4167.271	Mg I	-1.600	35051.263	
	4167.299	Fe II	-0.560	90300.626	
4171.02	4171.033	Mn II	-2.340	49425.654	
4171.86	4171.903	Cr II	-2.380	25042.811	
	4171.904	Ti II	-0.290	20951.754	
4172.05	4172.122	Fe I	-0.900	26224.966	
4173.50	4173.450	Fe II	-2.160	20830.553	
	4173.537	Ti II	-2.000	8744.250	
4174.27	4174.265	S II	0.800	140319.232	
4175.76	4175.83	Fe II		90487.827	
4176.60	4176.566	Fe I	-0.620	27166.817	
	4167.599	Mn I	-0.120	34138.880	
4177.66	4177.530	Y II	-0.160	3298.808	9 % line
	4177.686	Fe II	-3.450	20518.744	
4178.73	4178.711	Fe I	-2.930	35856.400	
4178.84	4178.855	Fe II	-2.440	20830.553	
4179.00	4179.054	V II	-2.500	13608.961	
4179.42	4179.421	Cr II	-1.800	30866.837	
	4179.393	Pr II	0.510	1649.010	
4179.54	4179.421	Cr II	-1.770	30864.459	
4179.70	4179.807	Zr II	-0.780	13428.500	
4181.58	4181.513	Cr II	-2.500	45730.581	
	4181.580	Fe II	-1.860	90898.872	
4181.75	4181.755	Fe I	-0.180	22838.320	

Table 1 continued on next page

Table 1 (*continued*)

λ_{obs} (Å)	λ_{lab} (Å)	Identification	$\log gf$	E_{low}	Comments
4183.28	4183.200	Fe I	-4.870	21308.040	broad absorbtion
4184.82	4184.867	Si II	-0.390	131677.039	
4186.99	4187.039	Fe I	-0.550	19757.031	
4187.81	4187.795	Fe I	-0.550	19562.437	
4188.89	4188.914	Fe II	-2.820	84863.353	
	4188.977	Fe II	-1.310	90780.619	
4190.70	4190.707	Si II	-0.330	108820.317	
4191.50	4191.430	Fe I	-0.670	19912.494	
4191.77	4191.750	Cr I	-2.500	20523.629	
4195.19	4195.184	Dy II	-0.360	9870.990	
4195.41	4195.417	Cr II	-2.320	42897.990	
4195.60	4195.618	Fe I	-1.800	24335.763	
4198.33	4198.304	Fe I	-0.720	19350.891	
4199.15	4199.095	Fe I	0.250	24574.655	
4200.77	4200.658	Si II	-0.890	101023.046	
	4200.778	Fe I	-4.030	12968.554	
4202.02	4202.029	Fe I	-0.710	11976.238	
4204.02	4203.965	Fe I	-1.010	26406.464	
4205.48	4205.48	Fe I	-5.380	29313.051	
	4205.381	Mn II	-3.380	14593.879	
4209.00	4208.977	Zr II	-0.460	5752.920	
4210.35	4210.343	Fe I	-0.870	20019.633	
4211.90	4211.907	Zr II	-1.080	4248.300	
4213.54	4213.518	Fe II	-2.210	62693.478	
4215.53	4215.519	Sr II	-0.170	0.000	15 % line
4217.43	4217.419	Ho III	-1.080	8645.000	
4219.39	4219.360	Fe I	0.120	19.952	
4222.09	4222.104	N I	-1.590	83317.031	
4222.44	4222.381	Zr II	-0.900	9742.800	
4224.96	4224.860	Cr II	-1.250	42989.353	very broad line
4226.73	4226.728	Ca I	0.240	0.000	resonance
4227.43	4227.427	Fe I	0.230	26874.546	

Table 1 continued on next page

Table 1 (*continued*)

λ_{obs} (Å)	λ_{lab} (Å)	Identification	$\log gf$	E_{low}	Comments
4233.15	4233.172	Fe II	-2.00	20830.582	21 % line
	4233.243	Cr II	-2.120	31168.581	
4235.95	4235.936	Fe I	-0.340	19562.437	
4238.82	4238.731	Mn II	-3.680	14781.170	
	4238.810	Fe I	-0.280	27394.689	
	4238.819	Fe II	-2.720	54902.315	
4242.39	4242.333	Mn II	-1.260	49820.159	
	4242.364	Cr II	-0.590	31219.350	
	4242.448	Mg II	-1.070	9330.590	
4244.90	4244.963	Nd II	-1.030	1650.205	
4246.85	4246.85	Sc II	0.320	2540.980	
4247.49	4247.425	Fe I	-0.230	27166.817	
4250.14	4250.119	Fe I	-0.410	19912.491	
4250.30	4250.359	Fe II	-6.150	79885.523	wrong gf ?
4250.74	4250.787	Fe I	-0.710	12560.933	
	4252.71	Cr II	-2.020	31117.390	
	4252.726	Fe II	-2.290	74606.841	
4252.71	4252.755	Fe II	-2.170	82853.660	
	4254.43	Cr I	-0.110	0.000	resonance
	4254.522	Cr II	-0.970	47354.440	
4528.21	4528.15	Fe II	-3.400	21812.055	
4259.06		Mn II			15 hfs
4259.27		Mn II			
4260.42	4260.467	Mn II	-4.250	14901.180	
	4260.474	Fe I	-0.020	19350.891	
4261.91	4261.913	Cr II	-1.530	31168.581	
	4261.847	Cr II	-3.000	25033.700	
4263.89	4263.869	Fe II	-1.710	62049.023	
	4263.849	V II	-2.680	13594.730	
4267.14	4267.001	C II	0.563	145549.27	
	4267.261	C II	0.716	145550.70	
	4267.261	C II	-0.584	145550.70	

Table 1 continued on next page

Table 1 (*continued*)

λ_{obs} (Å)	λ_{lab} (Å)	Identification	$\log gf$	E_{low}	Comments
4269.28	4269.277	Cr II	-2.170	31082.940	
4271.134	4271.153	Fe I	-0.350	19757.031	13 % blend
4271.80	4271.750	Fe I	-0.160	11976.238	
4273.24	4273.326	Fe II	-3.260	21812.055	
4273.38	4273.326	Fe II	-3.260	21812.055	
4274.76	4274.797	Cr I	-0.230	0.000	resonance
4275.61	4275.606	Cr II	-1.710	31117.390	
4278.20	4278.159	Fe II	-3.820	21711.917	
4282.45	4282.403	Fe I	-0.810	17550.180	
	4282.490	Mn II	-1.680	44521.521	
4284.35	4284.429	Mn II	-2.270	43311.301	
4287.91	4287.940	Fe I	-2.110	27666.345	
	4287.872	Ti II	-2.020	8710.440	
4289.50	4289.58	Mn II	-2.266	43339.452	
4290.66	4290.624	Fe I	-4.660	29313.005	wrong gf ?
4294.06	4294.099	Ti II	-1.110	8794.250	
	4294.125	Fe I	-1.110	11976.238	
4296.59	4296.572	Fe II	-3.010	21812.055	
4299.18	4299.234	Fe I	-0.430	19562.437	
4301.93	4301.914	Ti II	-1.160	9363.620	
4302.08	4302.186	Fe I	-1.740	24574.652	
4303.17	4303.176	Fe II	-2.490	21812.055	16 % line
4305.38	4305.443	Sr II	-0.140	24516.650	
	4305.450	Fe I	-1.300	24335.763	
4307.87	4307.863	Ti II	-1.290	9393.710	
	4307.902	Fe I	-0.070	12560.933	
4309.50	4309.631	Y II	-0.750	1449.808	
4312.87	4312.864	Ti II	-1.160	5518.060	
4313.89	4313.957	Fe II	-6.588	104315.373	wrong gf
4314.18		Sc II			5 hfs
4314.97	4314.975	Ti II	-1.130	9363.620	
	4314.979	Fe II	-3.100	38164.195	

Table 1 continued on next page

Table 1 (*continued*)

λ_{obs} (Å)	λ_{lab} (Å)	Identification	$\log gf$	E_{low}	Comments
4316.75	4316.799	Ti II	-1.420	16615.060	
4320.75	4320.725	Sc II	-0.260	4883.370	
4325.20	4325.176	Fe I	-1.580	24338.766	
4325.73	4325.762	Fe I	-0.010	12968.554	
	4325.758	Nd II	0.010	3801.990	
4351.81	4351.769	Fe II	-2.100	21812.055	
	4351.811	Cr I	-0.440	8307.577	
4357.56	4357.584	Fe II	-2.110	49100.978	
4359.75	4359.720	Zr II	-0.460	9968.650	
	4359.786	Fe II	-2.590	50212.823	
4362.11	4362.099	Ni II	-2.720	32499.529	broad blend
4368.05	4368.03	Sm II	-1.110	3052.690	
4369.45	4369.411	Fe II	-3.670	22469.852	
4371.29	4371.27	Cr I	-1.090	8095.1842	
4374.35	4374.426	Cr I	-4.737	27703.777	wrong gf
4374.74	4374.765	Dy II	-1.100	4341.100	
	4374.815	Ti II	-1.290	16625.110	
4375.03	4374.965	Y II	0.160	3296.184	
4383.62	4383.545	Fe I	0.200	11976.238	
4384.52	4384.637	Mg II	-0.790	80619.500	
4385.38	4385.387	Fe II	-2.570	22409.852	
4386.86	4386.844	Ti II	-1.260	20951.600	
4388.10	4388.078	Mn I	-1.250	38120.18	
4390.55	4390.514	Mg II	-1.490	80550.022	
	4390.572	Mg II	-0.530	80550.022	
4394.07	4394.051	Ti II	-1.590	9850.900	
4395.08	4395.033	Ti II	-0.660	8744.250	15 %
4395.86	4395.817	Fe II	-1.200	90487.811	
	4395.850	Ti II	-2.170	10024.730	
4399.73	4399.772	Ti II	-1.270	9975.920	
4400.50	4400.379	Sc II	-0.510	4883.570	
4401.61	4401.68	Cr II	-1.430	7103.000	?

Table 1 continued on next page

Table 1 (*continued*)

λ_{obs} (Å)	λ_{lab} (Å)	Identification	$\log gf$	E_{low}	Comments
4402.99	4403.033	Fe II	-4.187	87759.062	wrong gf
4404.75	4404.750	Fe I	-0.140	12560.933	10 % line
	4404.750	Zr II	-1.100	14739.350	
4409.50	4409.516	Ti II	-2.570	9930.690	
4411.08	4411.074	Ti II	-1.050	24961.031	
4413.67	4413.601	Fe II	-3.870	21581.638	
4415.17	4415.122	Fe I	-0.620	12968.354	
4416.78	4416.830	Fe II	-2.600	22409.852	
4416.89	4416.830	Fe II	-2.600	22409.852	
4417.69	4417.719	Ti II	-1.435	9395.710	
4418.37	4418.330	Ti II	-2.460	9975.920	
4421.92	4421.938	Ti II	-1.779	16625.110	
4425.46	4425.53	Fe I	-6.806	5999.394	wrong gf
4427.28	4427.298	Fe I	-1.250	42225.410	
	4427.310	Fe I	-3.040	415.933	
4427.95	4427.994	Mg II	-1.210	80619.500	
4430.56	4430.614	Fe I	-1.660	17927.381	
4434.03	4433.988	Mg II	-0.910	80550.022	
	4434.067	Mn II	-1.510	53017.157	
4434.98	4434.957	Ca I	-0.030	15210.063	
4443.00	4443.008	Zr II	-0.420	11984.460	
4443.84	4443.794	Ti II	-0.700	8710.440	
4444.50	4444.539	Fe II	-2.530	50157.455	
	4444.558	Ti II	-2.030	8997.710	
4447.50	4447.504	Fe II	-0.920	90397.870	
4449.60	4449.646	Fe II	-1.590	63948.792	
4450.49	4450.482	Ti II	-1.450	8744.250	broad
4451.52	4451.551	Fe II	-1.840	49506.935	
4451.62	4451.606	Mn I	0.280	2328.670	
4454.60	4454.629	Sm II	-0.590	4386.030	
4455.03	4455.031	Mn I	-0.390	24779.319	
4455.25	4455.266	Fe II	-2.140	50212.823	

Table 1 continued on next page

Table 1 (*continued*)

λ_{obs} (Å)	λ_{lab} (Å)	Identification	$\log gf$	E_{low}	Comments
4455.68	4455.621	Fe I	-1.160	36766.964	
4456.48	4456.465	Fe II	-1.120	91048.254	
4457.26	?				
4459.09	4459.117	Fe I	-1.280	17550.180	
	4459.027	Ni I	-0.150	26665.902	
4461.55	4461.653	Fe I	-3.210	704.007	
4464.53	4464.450	Ti II	-2.080	9363.620	
4466.60	4466.551	Fe I	-0.590	22838.320	
4468.51	4468.507	Ti II	-0.600	9118.260	15 % blend
4469.32	4469.376	Fe I	-0.260	29469.023	
4471.54	4471.473	He I	-0.280	169086.867	
	4471.488	He I	-0.550	169086.943	
4472.91	4472.929	Fe II	-3.450	22939.350	
4476.12	4476.068	Fe I	-2.700	26623.794	
4478.62	4478.637	Mn II	-0.950	53597.132	
4481.24	4481.126	Mg II	0.749	71490.190	
	4481.150	Mg II	-0.553	71490.190	
	4481.325	Mg II	0.594	71491.060	
4484.25	4484.220	Fe I	-0.720	29056.322	
4484.91	4489.921	Fe II	-7.500	16369.360	wrong $\log(gf)$?
4488.33	4488.33	Ti II	-0.820	25192.791	
4489.18	4489.179	Ca II	-0.618	68056.699	10 %
	4489.179	Ca II	-0.730	68056.699	
	4389.183	Fe II	-1.970	22810.356	
4491.46	4491.405	Fe I	-2.700	23031.299	
4493.58	4493.512	Ti II	-2.780	8710.440	
	4493.529	Fe II	-1.430	63876.319	
4494.65	4494.563	Fe I	-1.140	17726.988	
	4494.523	Ho III	-1.360	0.000	
4496.91	4496.980	Zr II	-0.890	57329.920	
	4496.986	Mn II	-0.860	85895.298	
4501.28	4501.273	Ti II	-0.750	8937.710	14 %

Table 1 continued on next page

Table 1 (*continued*)

λ_{obs} (Å)	λ_{lab} (Å)	Identification	$\log gf$	E_{low}	Comments
4508.24	4508.288	Fe II	-2.210	23031.299	
4515.34	4515.339	Fe II	-2.480	22939.357	
4518.40	4518.327	Ti II	-2.550	8710.440	
4520.24	4520.224	Fe II	-2.600	22637.205	blend
	4520.244	Fe I	-2.500	24772.016	
4522.65	4522.634	Fe II	-2.030	22939.357	15 % line
	4522.602	Eu II	-0.680	1669.210	
	4522.636	Eu II	-0.680	1669.210	
	4522.658	Eu II	-0.680	1669.210	
4525.05	4525.034	Fe II	-3.060	50075.928	
	4525.137	Fe I	-0.340	29056.322	
4526.492	4526.489	Fe II	-1.430	90901.125	
4528.49	4528.473	Ce II	0.070	6967.547	
	4528.503	V II	-1.310	33500.854	
	4528.614	Fe I	-0.822	17550.181	
4529.48	4529.569	Fe II	-3.190	44929.519	
4534.04	4533.969	Ti II	-0.770	9975.920	20 % line
4539.60	4539.608	Cr II	-2.530	32603.400	
4541.55	4541.524	Fe II	-3.050	23031.299	9 % line
4545.04	4545.133	Ti II	-1.870	9118.260	
	4545.148	Fe II	-2.460	62689.878	
4549.53	4549.474	Fe II	-1.750	22810.356	33 % line
	4549.617	Ti II	-0.450	12774.689	
4554.01	4554.033	Ba II	0.140	0.000	10 % line, 15 hfs iso
4554.99	4555.027	Fe I	-1.090	31307.244	
4555.94	4555.846	Fe II	-4.120	32277.322	
	4555.887	Ca I	-0.540	15315.940	
4558.66	4558.650	Cr II	-0.660	32854.311	
4563.69	4563.761	Ti II	-0.960	9850.900	
4565.76	4565.740	Cr II	-2.110	32603.400	
4571.98	4571.968	Ti II	-0.330	12676.970	15 % line
4576.36	4576.340	Fe II	-3.040	22439.357	7 % line

Table 1 continued on next page

Table 1 (*continued*)

λ_{obs} (Å)	λ_{lab} (Å)	Identification	$\log gf$	E_{low}	Comments
4579.80	4579.86	Co I	-2.657	54561.681	blend
4582.88	4582.835	Fe II	-3.100	22939.357	
4583.85	4583.837	Fe II	-2.020	22637.205	20 % line
4588.20	4588.199	Cr II	-0.630	32836.680	
4590.03	4589.958	Ti II	-1.790	9975.920	
	4589.967	O I	-2.290	86631.453	
4592.10	4592.049	Cr II	-1.220	32854.949	
4593.87	4593.807	Cr II	-4.920	23317.632	
4596.05	4596.015	Fe II	-1.840	30212.823	
4598.56	4598.494	Fe II	-1.500	62945.040	
4600.26	4600.627	Ti II	-3.620	10024.730	wrong gf ?
4604.99	4605.06	Cr I	-3.361	42261.229	
4616.64	4616.629	Cr II	-1.290	32844.760	
4618.84	4618.803	Cr II	-1.110	32854.949	
4620.52	4620.521	Fe II	-3.280	22810.356	
4621.78	4621.722	Si II	-0.380	101024.439	
4625.90	4625.893	Fe II	-2.200	48039.077	
4629.29	4629.279	Ti II	-2.240	9518.060	
	4629.339	Fe II	-2.370	22637.205	13 %
4634.98	4634.070	Cr II	-1.240	32844.760	
4635.22	4635.316	Fe II	-1.650	48039.087	
4638.18	4638.050	Fe II	-1.520	62171.614	
4648.90	4648.944	Fe II	-4.390	20830.582	
4654.48	4654.498	Fe I	-2.780	12560.953	
4657.10	4656.981	Fe II	-3.630	23317.632	
	4657.206	Ti II	-2.150	10024.730	
4663.06	4663.046	Al II	-0.280	85481.548	
4663.77	4663.708	Fe II	-4.270	23317.632	
4665.72	4665.79	Fe II	-4.860	21812.045	wrong gf ?
4666.72	4666.758	Fe II	-3.330	22810.356	
4670.17	4670.182	Fe II	-4.100	20830.582	
4679.07	4679.159	Ni II	-1.750	56371.411	

Table 1 continued on next page

Table 1 (*continued*)

λ_{obs} (Å)	λ_{lab} (Å)	Identification	$\log gf$	E_{low}	Comments
4702.95	4702.991	Mg I	-0.670	35051.263	
	4702.991	Zr II	-0.800	20080.301	
4707.37	4707.382	Ti II	-4.170	42208.591	
4708.66	4708.665	Ti II	-2.210	9375.920	
	4708.750	Fe II	-2.350	78577.282	
4714.41	4714.410	Mn II	-3.550	14593.819	
4736.82	4736.773	Fe I	-0.740	25899.986	
4731.45	4731.453	Fe II	-3.360	23317.632	
4755.78	4755.727	Mn II	-1.240	43528.639	
4762.58	4762.538	C I	-2.440	60352.630	
4764.71	4764.738	Mn II	-1.350	43357.156	
4770.00	4770.027	C I	-2.720	60352.630	
4771.73	4771.742	C I	-2.120	60393.138	
4775.89	4775.897	C I	-2.160	60393.138	
4780.06	4779.985	Ti II	-1.370	16518.860	
4786.57	4786.580	Y II	-1.290	8328.041	
4805.07	4805.085	Ti II	-1.100	16625.110	
4812.46	4812.468	Fe I	-5.400	22249.428	wrong gf ?
4824.15	4824.126	Cr II	-1.220	31219.350	10 % line
4836.14	4836.229	Cr II	-2.250	31117.390	
4848.25	4848.235	Cr II	-1.140	31168.581	
4876.47	4876.399	Cr II	-1.460	31082.940	
	4876.473	Cr II	-1.460	31168.581	
4883.67	4883.684	Y II	0.070	8743.816	
4890.87	4890.755	Fe I	-0.430	23192.497	
4891.53	4891.492	Fe I	-0.140	22996.673	
	4891.485	Cr II	-3.040	31350.901	
4900.17	4900.120	Y II	-0.090	8328.041	
4911.23	4911.193	Ti II	-0.340	25192.791	
4919.01	4918.994	Fe I	-0.370	23110.937	
	4918.954	Fe I	-0.340	33507.120	
4920.57	4920.502	Fe I	0.060	22845.868	

Table 1 continued on next page

Table 1 (*continued*)

λ_{obs} (Å)	λ_{lab} (Å)	Identification	$\log gf$	E_{low}	Comments
4922.14	4922.192	Fe II	-0.800	83558.539	
4923.96	4924.030	Fe II	-1.321	23317.632	20 % line
4932.10	4932.049	C I	-1.880	61981.822	
	4932.080	Fe II	-1.730	83196.488	
4934.11	4934.076	Ba II	-0.150	0.000	resonance
4951.62	4951.584	Fe II	0.180	83136.488	
4957.65	4957.596	Fe I	0.130	22650.014	very broad blend
	4957.692	Fe I	-0.330	33801.571	
4967.97	4967.897	Fe I	-0.530	33811.571	
4968.77	4968.698	Fe I	-1.780	29356.743	
4982.59	4982.499	Fe I	0.160	33095.940	
4984.30	4984.276	Mn II	-3.270	94886.504	wrong gf ?
4990.38	4990.441	Cr II	-2.380	47354.440	wrong gf ?
4990.73	4990.768	Fe II	-3.850	64831.941	wrong gf ?
4991.26	4991.268	Fe I	-0.670	33801.571	
	4991.326	C I	-2.470	69744.032	
4992.11	4992.093	Mn II	-3.670	86936.810	wrong gf ?
4993.53	4993.680	Fe I	-1.450	33946.933	
5001.88	5001.863	Fe I	0.010	31307.244	
	5001.959	Fe II	0.900	82853.660	
5004.16	5004.195	Fe II	0.500	82853.660	
5006.86	5006.841	Fe II	-0.430	83713.596	
5007.55	5007.447	Fe II	-0.360	83726.362	
5010.04	5010.06	Fe II	-0.850	83726.362	
5013.93	5014.042	S II	0.030	113461.337	
5015.52	5015.520	Fe II	-2.520	73395.932	
5018.45	5018.440	Fe II	-1.220	23337.033	20 %
5019.95	5019.971	Ca II	-0.260	60611.279	
	5020.015	Fe II	-0.720	22978.679	
5022.54	5022.583	Fe II	-4.040	44929.549	
5030.81	5030.89	Fe II	-1.772	104588.729	
5032.72	5032.712	Fe II	0.110	83812.217	

Table 1 continued on next page

Table 1 (*continued*)

λ_{obs} (Å)	λ_{lab} (Å)	Identification	$\log gf$	E_{low}	Comments
5040.94	5040.907	Fe I	-0.500	34547.209	
	5041.024	Si II	0.290	81191.341	
5047.75	5047.641	Fe II	-0.070	83136.488	
	5047.783	O I	-2.520	88631.144	
	5047.823	O I	-3.220	88631.302	
5048.78	5048.843	Ni I	-0.380	31031.041	
5052.15	5052.167	C I	-1.650	61981.822	
5056.11	5056.194	Ni II	0.500	99154.808	
5056.81	5056.718	Fe II	0.220	83136.488	broad blend
5065.10	5065.018	Fe I	-0.450	34328.750	
	5065.097	Fe II	-0.450	84131.564	
	5065.193	Fe I	-1.510	29371.811	
5070.70	5070.78	Co I	-3.341	55165.690	
5080.60	5080.528	Ni I	0.130	29481.020	
5082.32	5082.230	Fe II	-0.100	83990.065	
5087.44	5087.416	Y II	-0.170	8743.316	
	5087.350	Fe II	-1.830	83459.671	
5093.47	5093.465	Fe II	-2.140	54870.528	
	5093.576	Fe II	0.110	83713.536	
5097.16	5097.270	Fe II	0.310	83713.536	
5098.81	5098.70	Fe I	-2.030	17550.181	
5100.49	5100.607	Fe II	0.170	83726.362	
5100.80	5100.852	Fe II	-1.780	47674.718	
	5100.727	Fe II	0.700	83726.362	
5129.18	5129.152	Ti II	-1.390	15257.430	
5133.81	5133.688	Fe I	0.140	33695.394	
5137.16	5137.088	Cr II	-1.530	55023.098	
5139.43	5139.462	Fe I	-0.570	23711.453	
5142.48	5142.486	Cr II	-2.190	50667.272	
	5142.541	Fe I	-0.140	34328.750	
5144.30	5144.355	Fe II	0.280	84424.372	
5146.08	5146.127	Fe II	-3.910	22810.356	

Table 1 continued on next page

Table 1 (*continued*)

λ_{obs} (Å)	λ_{lab} (Å)	Identification	$\log gf$	E_{low}	Comments
5149.42	5149.465	Fe II	0.400	84266.557	
5154.10	5154.070	Ti II	-1.920	12628.731	
5157.36	5157.282	Fe II	-0.310	84236.910	
5160.84	5160.839	Fe II	-2.640	44915.046	
5162.84	5162.92	N I	-1.405	94881.820	
5167.37	5167.321	Mg I	-1.030	21850.405	12 %
	5167.488	Fe I	-1.260	11976.238	
5169.07	5169.033	Fe II	-0.870	23317.632	20 %
5171.54	5171.596	Fe I	-1.790	11976.238	
	5171.640	Fe II	-4.370	22637.205	
5172.73	5172.684	Mg I	-0.400	21870.163	15 %
5177.21	5177.333	Fe I	-2.420	29798.933	
5180.14	5180.170	Fe I	-1.230	40257.311	
5183.52	5183.600	Mg I	-0.180	21911.173	18 %
5185.80	5185.902	Ti II	-1.350	15265.701	3 %
5188.77	5188.69	Ti II	-1.210	12758.260	7 %
5191.52	5191.454	Fe I	-0.550	24506.914	
5192.50	5192.442	Fe II	-2.020	5192.442	
5195.00	5195.124	Pr II	-0.130	8950.490	broad
5196.30	5196.44	Fe II	-1.020	83713.536	
5197.59	5197.577	Fe II	-2.100	26055.422	10 %
	5197.480	Fe II	-2.720	48039.087	
	5197.577	Fe I	-2.320	39969.851	
5199.15	5199.122	Fe II	0.100	3713.536	
5205.74	5205.724	Y II	-0.340	8328.041	
5208.88	5208.425	Cr I	0.160	7593.150	
5210.64	5210.626	Fe I	-3.580	39625.801	wrong gf ?
5211.39	5211.47	Mn I	-7.870	47212.078	wrong gf
5213.57	5213.540	Fe II	-0.820	84870.863	
5215.48	5215.349	Fe II	-0.010	83713.536	
5216.83	5216.814	Fe II	-0.230	83726.362	
5226.84	5226.862	Fe I	-0.550	24506.914	broad

Table 1 continued on next page

Table 1 (*continued*)

λ_{obs} (Å)	λ_{lab} (Å)	Identification	$\log gf$	E_{low}	Comments
	5226.897	Fe I	-1.250	34636.789	
	5226.899	Cr I	-2.010	27222.944	
5227.41	5227.481	Fe II	0.800	84296.829	7 % broad
	5227.323	Fe II	-0.030	84344.832	
5232.85	5232.787	Fe II	-0.060	83726.362	5 %
	5232.940	Fe I	-0.190	2378.453	
5234.59	5234.625	Fe II	-2.250	25981.630	10 %
5237.29	5237.329	Cr II	-1.150	32854.311	5 %
5247.95	5247.952	Fe II	0.630	84938.177	
5249.39	5249.344	Fe II	-0.600	83930.015	
	5249.437	Cr II	-2.430	30307.439	
5251.26	5251.233	Fe II	0.510	84844.832	
	5251.211	Fe II	-0.850	84236.910	
5253.55	5253.479	P II	0.290	85893.219	
	5253.514	Fe II	-1.100	84296.829	
	5253.641	Fe II	-0.090	84296.829	
5254.12	5234.140	Cr I	-1.950	35397.270	
5257.09	5257.122	Fe II	0.030	84685.198	
5260.29	5260.259	Fe II	-1.070	84035.139	
5264.10	5264.177	Fe II	0.360	84710.686	
5264.59	5264.697	Fe II	-2.810	65696.036	
5266.55	5266.555	Fe I	-0.490	24180.861	
5266.87	5266.957	Co I	-7.244	57813.258	wrong gf
5269.70	5269.537	Fe I	-1.320	6928.268	
5270.30	5270.356	Fe I	-1.510	12968.554	
5272.32	5272.337	Fe II	-2.030	48039.087	
5275.01	5274.964	Cr II	-1.29	32836.680	
5276.11	5276.002	Fe II	-1.940	25805.329	12 %
5279.99	5279.876	Cr II	-2.100	32851.311	
	5280.054	Cr II	-2.010	32854.949	
5280.13	5280.054	Cr II	-2.010	32834.949	
5281.62	5281.63	Fe I		4059.432	

Table 1 continued on next page

Table 1 (*continued*)

λ_{obs} (Å)	λ_{lab} (Å)	Identification	$\log gf$	E_{low}	Comments
5281.93	5282.01	Fe II	-2.795	108929.031	
5283.33	5283.44	Ti II		12156.802	
5283.94	5284.109	Fe II	-3.190	23317.632	5 %
5291.66	5291.666	Fe II	0.58	84527.779	
5294.00	5294.086	Fe I	-0.660	40842.150	
	5294.099	Nd III	-0.650	0.000	resonance
5299.20	5299.30	Mn II	-0.420	79558.538	
5302.35	5302.300	Fe I	-0.880	26479.378	
	5302.342	Mn II	-0.820	79569.268	
	5302.402	Mn II	0.230	79569.268	
	5302.431	Mn II	1.000	79569.268	
5305.99	5306.180	Fe II	0.220	84870.863	
	5305.929	Cr II	0.110	86732.041	
5307.22	5307.224	Ca II	-0.850	60611.179	
5308.36	5308.408	Cr II	-1.810	32836.680	
5310.65	5310.635	Fe II	-0.860	84527.779	
	5310.687	Cr II	-2.880	32844.700	
5313.57	5313.563	Cr II	-1.650	32854.949	
5316.63	5316.615	Fe II	-1.850	25428.783	20 % line
5324.14	5324.179	Fe I	-0.240	25899.986	
5325.50	5325.503	Fe II	-2.800	25981.670	
5328.11	5328.039	Fe I	-1.470	7376.64 0	
5328.90	5328.934	Fe II	-0.790	84938.177	
5329.68	5329.673	O I	-2.200	86627.777	
		O I	-1.610	86627.777	
		O I	-1.410	86627.777	
5330.73	5330.741	O I	-1.120	86631.453	
5334.85	5334.869	Cr II	-1.560	32844.760	
5336.80	5336.88	V II	-4.058	216464.20	wrong gf
5337.80	5337.732	Fe II	- 3.890	26055.422	
	5337.772	Cr II	-2.030	32854.949	
5339.57	5339.585	Fe II	0.540	84296.829	

Table 1 continued on next page

Table 1 (*continued*)

λ_{obs} (Å)	λ_{lab} (Å)	Identification	$\log gf$	E_{low}	Comments
5362.92	5362.869	Fe II	-2.740	25805.329	10 % line
	5362.957	Fe II	-0.080	84685.798	
5364.78	5364.871	Fe I	0.220	53856.400	
5367.44	5367.466	Fe I	0.350	35611.622	
5370.11	5369.961	Fe I	0.350	35257.323	
	5370.164	Cr II	0.320	86782.011	
5371.42	5371.489	Fe I	-1.650	7728.059	
	5371.437	Fe I	-1.240	35767.561	
5380.68	5380.786	Cr II	-0.700	86980.102	
5381.08	5381.015	Ti II	-2.080	12628.731	
5383.39	5383.369	Fe I	0.500	34782.420	
5387.02	5387.063	Fe II	0.520	84863.353	
5395.82	5395.857	Fe II	0.360	85495.303	
	5395.751	Cr II	0.910	86980.102	
5401.90	5402.059	Fe II	0.500	85184.734	
5404.11	5404.117	Fe I	0.540	34782.420	
	5404.151	Fe I	0.520	35767.561	
5405.67	5405.663	Fe II	-0.440	48708.863	
	5405.775	Fe I	-1.840	7985.784	
5407.40	5407.604	Cr II	-2.090	30864.459	
5408.30	5408.373	Ti I	-3.007	43592.120	wrong gf
5411.05	5410.910	Fe I	0.280	36079.371	
5414.56	5414.850	Fe II	-0.310	84863.359	broad blend
	5414.862	Cr II	-1.780	55023.098	
	5414.925	Fe II	-2.290	83130.901	
5424.17	5424.068	Fe I	0.320	34843.954	
5425.07	5425.257	Fe II	-3.360	25805.329	
5427.90	5428.826	Fe II	-1.660	54232.193	
5429.87	5429.988	Fe II	0.460	85462.859	
5433.00	5432.967	Fe II	-3.630	26352.767	
5433.67	5433.643	Fe I	-0.840	40871.951	
5434.36	5434.315	Mn II	-2.040	84307.200	

Table 1 continued on next page

Table 1 (*continued*)

λ_{obs} (Å)	λ_{lab} (Å)	Identification	$\log gf$	E_{low}	Comments
5435.14	5435.178	O I	-1.880	86625.757	
5436.68	5436.618	Fe II	-0.950	85048.600	
5455.54	5455.454	Fe I	0.300	34843.954	
	5455.462	Dy II	-0.541	9492.000	
5465.99	5465.931	Fe II	0.520	85679.698	
5466.90	5466.908	Fe II	-1.880	54902.319	
	5466.894	Si II	-0.040	101024.349	
5481.18	5481.24	Fe I	-1.400	33095.941	
	5481.27	Fe II	-1.210	85462.937	
5482.21	5482.308	Fe II	0.430	85184.734	
5487.53	5487.619	Fe II	0.360	85462.859	
5492.05	5492.033	Fe II	-0.900	85495.303	
	5492.079	Fe II	-0.180	85679.698	
5493.86	5493.833	Fe II	0.210	81685.198	
	5493.876	Fe I	-0.620	45293.630	
5502.08	5502.067	Cr II	-1.990	33618.940	
5503.28	5503.211	Fe II	-0.090	8468.514	
	5503.212	Cr II	-2.310	33417.990	
	5503.358	Fe II	-0.591	85495.303	
5506.25	5506.195	Fe II	0.950	84863.353	
5508.72	5508.610	Cr II	-2.110	33521.110	broad
5510.66	5510.639	Fe II	-1.000	85184.734	
	5510.702	Cr II	-2.450	30864.459	
	5510.779	Fe II	0.000	85184.734	
5525.34	5525.43	Fe II	-4.255	105630.764	wrong gf
5526.86	5526.770	Sc II	0.130	14261.320	
5528.50	5528.405	Mg I	-0.620	35051.263	
5529.92	5529.932	Fe II	-1.870	54273.640	
5534.83	5534.847	Fe II	-2.940	26170.181	5 %
	5534.890	Fe II	-0.690	85048.620	
5544.70	5544.763	Fe II	0.128	84863.353	
5549.00	5549.001	Fe II	-0.230	84870.863	

Table 1 continued on next page

Table 1 (*continued*)

λ_{obs} (Å)	λ_{lab} (Å)	Identification	$\log gf$	E_{low}	Comments
5567.95	5567.842	Fe II	-1.890	54283.218	
5569.58	5569.617	Cr II	0.080	87948.549	
	5569.618	Fe I	-0.540	27559.582	
5572.84	5572.842	Fe II	-0.310	27394.689	
5576.00	5575.967	Si II	-1.670	103885.252	
	5575.980	cr II	-0.100	87666.259	
	5576.089	Fe I	-1.000	27666.345	
5578.00	5577.915	Fe II	-0.140	85462.859	
	5577.997	Fe II	-0.610	85495.303	
5586.79	5586.842	Cr II	0.910	88001.361	
	5586.756	Fe I	-0.210	27166.817	
5588.61	5588.619	Cr II	-5.550	31117.390	wrong gf
5594.44	5594.462	Ca I	-0.050	20349.261	
	5594.563	Fe II	-1.130	85495.303	
5598.30	5598.287	Fe I	-0.370	37521.157	
5603.12	5603.065	Mn I	-2.400	35041.370	?
5615.69	5615.644	Fe I	-0.140	26874.547	
5643.92	5643.880	Fe II	-1.460	61726.078	asymmetric
5662.74	5662.93	Y II	0.340	15682.898	
5748.28	5748.286	Fe II	-0.680	87471.765	
5813.66	5813.677	Fe II	-2.750	44929.549	
5851.34	5851.442	V II	-0.960	73530.712	
6024.27	6024.178	P II	0.140	86743.961	
6103.49	6103.496	Fe II	-2.170	50142.788	
6141.64	6141.713	Ba II	-0.030	5674.824	broad
	6141.731	Fe I	-1.610	29056.322	
6147.62	6147.741	Fe II	-2.720	31364.440	
6149.26	6149.258	Fe II	-2.720	31968.450	
6155.87	6155.961	O I	-1.400	86625.757	
	6155.971	O I	-1.050	86625.757	
	6155.989	O I	-1.160	86625.757	
6156.62	6156.737	O I	-1.520	86627.777	

Table 1 continued on next page

Table 1 (*continued*)

λ_{obs} (Å)	λ_{lab} (Å)	Identification	$\log gf$	E_{low}	Comments
	6156.755	O I	-0.930	86627.777	
	6156.778	O I	-0.730	86627.777	
6158.17	6158.149	O I	-1.890	86631.453	
	6158.172	O I	-1.030	86631.453	
	6158.187	O I	-0.440	86631.453	
6175.26	6175.146	Fe II	-1.980	50187.813	
6233.61	6233.534	Fe II	-2.340	44232.513	
6238.37	6238.392	Fe II	-2.630	31364.440	5 %
6239.66	6239.614	Si II	0.190	103556.025	
	6239.665	Si II	0.080	103556.156	
6247.61	6247.557	Fe II	-2.330	31307.949	
6347.12	6347.109	Si II	0.300	65500.472	
6371.48	6371.371	Si II	0.000	65500.472	
6383.61	6383.722	Fe II	-2.270	44784.760	
6390.04					?
6416.90	6416.919	Fe II	-2.740	31387.949	blend
6419.85	6419.949	Fe I	-0.240	38175.351	asymmetric
6432.48	6432.680	Fe II	-3.710	23317.632	
6453.56	6453.602	O I	-1.360	86625.757	
6456.47	6456.383	Fe II	-2.070	31483.167	10 %

Table 2. Elemental Abundances from unblended lines for HR 8844. References are defined in Tab. 5.

Element	λ (Å)	$\log gf$	Ref.	$\log(X/H)_{HR8844}$	$\log(X)_{\odot}$	$\log(X)_{\odot} - 12$
He I	4471.470	-2.211	NIST/ASD	-1.37	10.93	-1.07
He I	4471.474	-0.287	NIST/ASD	-1.37		
He I	4471.474	-1.035	NIST/ASD	-1.37		
He I	4471.485	-1.035	NIST/ASD	-1.37		
He I	4471.489	-0.558	NIST/ASD	-1.37		
He I	4471.683	-0.910	NIST/ASD	-1.37		
He I	5875.598	-1.516	NIST/ASD	-1.22		
He I	5875.613	-0.339	NIST/ASD	-1.22		
He I	5875.615	0.409	NIST/ASD	-1.22		
He I	5875.625	-0.339	NIST/ASD	-1.22		
He I	5875.640	0.138	NIST/ASD	-1.22		
He I	5875.966	-0.214	NIST/ASD	-1.22		
$\log(He/H) = -1.30 \pm 0.45$ dex $[\frac{He}{H}] = -0.23 \pm 0.45$ dex						
C II	4267.261	0.716	NIST/ASD	-3.88	8.52	-3.48
C II	4267.261	-0.584	NIST/ASD	-3.88		
$\log(C/H) = -3.88 \pm 0.34$ dex $[\frac{C}{H}] = -0.40 \pm 0.34$ dex						
O I	5330.726	-2.416	NIST/ASD	-3.27	8.83	-3.17
O I	5330.741	-0.983	NIST/ASD	-3.27		
O I	6155.961	-1.363	NIST/ASD	-3.26		
O I	6155.971	-1.011	NIST/ASD	-3.26		
O I	6155.989	-1.120	NIST/ASD	-3.26		
O I	6156.737	-1.487	NIST/ASD	-3.26		
O I	6155.755	-0.898	NIST/ASD	-3.26		
O I	6156.778	-0.694	NIST/ASD	-3.26		
O I	6158.149	-1.841	NIST/ASD	-3.26		
O I	6158.172	-0.995	NIST/ASD	-3.26		
O I	6158.187	-0.409	NIST/ASD	-3.26		
$\log(O/H) = -3.27 \pm 0.19$ dex						

Table 2 continued on next page

Table 2 (*continued*)

Element	λ (Å)	$\log gf$	Ref.	$\log(X/H)_{HR8844}$	$\log(X)_{\odot}$	$\log(X)_{\odot} - 12$
$\left[\frac{O}{H}\right] = -0.09 \pm 0.19$ dex						
Mg II	4390.572	-0.523	NIST/ASD	-4.72	7.58	-4.42
Mg II	4427.994	-1.208	NIST/ASD	-4.82		
$\log(Mg/H) = -4.77 \pm 0.29$ dex $\left[\frac{Mg}{H}\right] = -0.35 \pm 0.29$ dex						
Al II	4663.056	-0.244	NIST/ASD	-5.53	6.47	-5.53
Al I	3944.006	-0.635	NIST/ASD	-5.75		
$\log(Al/H) = -5.64 \pm 0.20$ dex $\left[\frac{Al}{H}\right] = -0.097 \pm 0.20$ dex						
Si II	4128.054	0.359	NIST/ASD	-4.60	7.55	-4.45
Si II	4130.894	0.552	NIST/ASD	-4.60		
Si II	4190.72	-0.351	Sh61	-4.60		
Si II	5041.024	0.029	NIST/ASD	-4.44		
Si II	5055.984	0.523	NIST/ASD	-4.52		
Si II	5056.317	-0.492	NIST/ASD	-4.52		
Si II	6371.37	-0.082	NIST/ASD	-4.27		
$\log(Si/H) = -4.51 \pm 0.09$ dex $\left[\frac{Si}{H}\right] = -0.06 \pm 0.09$ dex						
S II	4153.06	0.395	NIST/ASD	-4.67	7.33	-4.67
S II	4162.31	0.161	NIST/ASD	-4.67		
S II	4162.67	0.830	NIST/ASD	-4.67		
$\log(S/H) = -4.67 \pm 0.16$ dex $\left[\frac{S}{H}\right] = 0.00 \pm 0.16$ dex						
Ca II	3933.663	0.135	NIST/ASD	-5.83	6.36	-5.64
$\log(Ca/H) = -5.83 \pm 0.17$ dex $\left[\frac{Ca}{H}\right] = -0.19 \pm 0.17$ dex						
Sc II	4246.822	0.242	NIST/ASD	-9.05	3.17	-8.83
Sc II	5031.021	-0.400	NIST/ASD	-8.98		
Sc II	5526.813	-0.77	NIST/ASD	-8.93		
$\log(Sc/H) = -8.99 \pm 0.28$ dex						

Table 2 continued on next page

Table 2 (*continued*)

Element	λ (Å)	$\log gf$	Ref.	$\log(X/H)_{HR8844}$	$\log(X)_{\odot}$	$\log(X)_{\odot} - 12$
$[\frac{Sc}{H}] = -0.16 \pm 0.28$ dex						
Ti II	4163.644	-0.128	NIST/ASD	-6.78	5.02	-6.98
Ti II	4287.873	-2.020	NIST/ASD	-6.98		
Ti II	4290.210	-0.848	NIST/ASD	-6.98		
Ti II	4300.042	-0.442	NIST/ASD	-6.68		
Ti II	4411.072	-0.6767	NIST/ASD	-6.78		
Ti II	4468.492	-0.620	NIST/ASD	-6.78		
Ti II	4563.758	-0.96	NIST/ASD	-6.78		
Ti II	5129.156	-1.239	NIST/ASD	-6.98		
Ti II	5188.687	-1.220	NIST/ASD	-6.87		
Ti II	5336.780	-1.700	NIST/ASD	-6.98		
$\log(Ti/H) = -6.83 \pm 0.06$ dex						
$[\frac{Ti}{H}] = 0.15 \pm 0.06$ dex						
V II	4005.71	-0.450	NIST/ASD	-7.77	4.00	-8.00
V II	4023.39	-0.610	K10/BGF/WLDS	-7.66		
V II	4036.78	-1.570	NIST/ASD	-7.70		
$\log(V/H) = -7.71 \pm 0.23$ dex						
$[\frac{V}{H}] = 0.29 \pm 0.23$ dex						
Cr II	4558.644	-0.660	NIST/ASD	-6.12	5.67	-6.33
Cr II	4558.787	-2.460	SN14	-6.12		
Cr II	5237.322	-1.160	NIST/ASD	-6.33		
Cr II	5308.421	-1.810	NIST/ASD	-6.18		
Cr II	5313.581	-1.650	NIST/ASD	-6.18		
Cr II	5502.086	-1.990	NIST/ASD	-6.12		
$\log(Cr/H) = -6.18 \pm 0.17$ dex						
$[\frac{Cr}{H}] = 0.16 \pm 0.17$ dex						
Mn II	4206.368	-1.54	NIST/ASD	-6.32	5.39	-6.61
$\log(Mn/H) = -6.32 \pm 0.08$ dex						
$[\frac{Mn}{H}] = 0.30 \pm 0.08$ dex						
Fe II	4258.148	-3.500	NIST/ASD	-4.65	7.50	-4.50

Table 2 continued on next page

Table 2 (*continued*)

Element	λ (Å)	$\log gf$	Ref.	$\log(X/H)_{HR8844}$	$\log(X)_{\odot}$	$\log(X)_{\odot} - 12$
Fe II	4273.326	-3.350	NIST/ASD	-4.62		
Fe II	4296.566	-2.900	NIST/ASD	-4.50		
Fe II	4491.397	-2.640	NIST/ASD	-4.50		
Fe II	4508.280	-2.300	NIST/ASD	-4.50		
Fe II	4515.333	-2.360	NIST/ASD	-4.50		
Fe II	4520.218	-2.600	NIST/ASD	-4.46		
Fe II	4923.921	-1.210	NIST/ASD	-4.35		
Fe II	5275.997	-1.900	NIST/ASD	-4.50		
Fe II	5316.609	-1.780	NIST/ASD	-4.42		
Fe II	5506.199	0.860	NIST/ASD	-4.50		
$\log(Fe/H) = -4.50 \pm 0.16$ dex $[\frac{Fe}{H}] = 0.00 \pm 0.16$ dex						
Ni II	4067.04	-1.834	K03	-6.05	6.25	-5.75
$\log(Ni/H) = -6.05 \pm 0.27$ dex $[\frac{Ni}{H}] = -0.30 \pm 0.27$ dex						
Sr II	4215.519	-1.610	NIST/ASD	-8.33	2.97	-9.03
$\log(Sr/H) = -8.33 \pm 0.18$ dex $[\frac{Sr}{H}] = 0.70 \pm 0.18$ dex						
Y II	3982.592	-0.560	NIST/ASD	-8.46	2.24	-9.16
Y II	5662.922	0.340	Bie11	-8.46		
$\log(Y/H) = -8.46 \pm 0.17$ dex $[\frac{Y}{H}] = 0.70 \pm 0.17$ dex						
Zr II	3998.965	-0.520	L06	-8.86	2.60	-9.40
Zr II	4442.992	-0.420	L06	-8.55		
Zr II	4457.431	-1.220	L06	-8.55		
Zr II	5112.270	-0.850	L06	-8.55		
$\log(Zr/H) = -8.63 \pm 0.17$ dex $[\frac{Zr}{H}] = 0.77 \pm 0.17$ dex						
Ba II	4934.077	-0.156	NIST	-8.87	2.13	-9.87
Ba II	6141.713	-0.032	NIST	-8.94		

Table 2 continued on next page

Table 2 (*continued*)

Element	λ (Å)	$\log gf$	Ref.	$\log(X/H)_{HR8844}$	$\log(X)_{\odot}$	$\log(X)_{\odot} - 12$
$\log(Ba/H) = -8.91 \pm 0.25$ dex						
$[\frac{Ba}{H}] = 0.97 \pm 0.25$ dex						
La II	4042.91	0.33	Zi99	-9.43	1.17	-10.83
$\log(La/H) = -9.43 \pm 0.25$ dex						
$[\frac{La}{H}] = 1.40 \pm 0.25$ dex						
Pr III	5299.99	-0.66	ISAN	-8.81	0.71	-11.29
$\log(Pr/H) = -8.81 \pm 0.25$ dex						
$[\frac{Pr}{H}] = 2.48 \pm 0.25$ dex						
Nd III	5265.019	-0.720	RRKB	-9.50	1.50	-10.50
$\log(Nd/H) = -9.50 \pm 0.25$ dex						
$[\frac{Nd}{H}] = 1.00 \pm 0.25$ dex						
Sm II	4424.32	0.14	LA06	-9.21	1.01	-10.99
$\log(Sm/H) = -9.21 \pm 0.25$ dex						
$[\frac{Sm}{H}] = 1.78 \pm 0.25$ dex						
Eu II	4129.70	-0.062	LWHS	-10.31	0.51	-11.49
$\log(Eu/H) = -10.31 \pm 0.25$ dex						
$[\frac{Eu}{H}] = 1.18 \pm 0.25$ dex						
Tb II	4005.47	-0.02	LA01	no conclusion	-0.1	-12.10
Ho II	4152.62	-0.93	LA04	-11.74 (ul)	0.26	-11.74
$\log(Ho/H) = -11.74 \pm 0.25$ dex						
$[\frac{Ho}{H}] = 0.00 \pm 0.25$ dex						
Er II	3906.31	0.12	LA08	-9.67	0.93	-11.07
$\log(Er/H) = -9.67 \pm 0.25$ dex						
$[\frac{Er}{H}] = 1.40 \pm 0.25$ dex						
Hg II	3983.931	hfs	Do03	-6.91	1.09	-10.91
$\log(Hg/H) = -6.91 \pm 0.23$ dex						
$[\frac{Hg}{H}] = 4.00 \pm 0.23$ dex						

Table 3. Elemental Abundances for the comparison stars ν Cap, ν Cnc, Sirius A and HD 72660

Element	λ (Å)	$\log(X/H)_{\nu Cap}$	$\log(X/H)_{\nu Cnc}$	$\log(X/H)_{Sirius}$	$\log(X/H)_{HD72660}$
He I	4471.470	-1.07	-1.47	-1.77	-2.07
He I	4471.474	-1.07	-1.47	-1.77	-2.07
He I	4471.474	-1.07	-1.47	-1.77	-2.07
He I	4471.485	-1.07	-1.47	-1.77	-2.07
He I	4471.489	-1.07	-1.47	-1.77	-2.07
He I	4471.683	-1.07	-1.47	-1.77	-2.07
He I	5875.598	-1.07	-1.47	-1.77	-2.07
He I	5875.613	-1.07	-1.47	-1.77	-2.07
He I	5875.615	-1.07	-1.47	-1.77	-2.07
He I	5875.625	-1.07	-1.47	-1.77	-2.07
He I	5875.640	-1.07	-1.47	-1.77	-2.07
He I	5875.966	-1.07	-1.47	-1.77	-2.07
Average He I		-1.07	-1.47	-1.77	-2.07
C II	4267.001	-3.48	-3.78		-4.00
C II	4267.261	-3.48	-3.78		-4.30
C II	4267.261	-3.48	-3.78		-4.30
C I	4932.041			-4.00	-4.00
C I	5052.15			-4.08	bl.
Average C		-3.48	-3.78	-4.04	-4.15
N I	4914.94	-4.02 (u.l)	-4.02 (u.l)	-4.02 (ul)	-4.02 (ul)
N I	4935.12	-4.02 (u.l)	-4.02 (u.l)	-4.02 (ul)	-4.02 (ul)
Average N I		-4.02	-4.02	-4.02	-4.02
O I	5329.673	-3.02	-3.22	-3.47	na
O I	5330.726	-3.02	-3.22	-3.44	na
O I	5330.741	-3.02	-3.22	-3.44	na
O I	6155.961	-3.02	-3.22	-3.63	-3.57
O I	6155.971	-3.02	-3.22	-3.63	-3.57
O I	6155.989	-3.02	-3.22	-3.63	-3.57
O I	6156.737	-3.02	-3.22	-3.63	-3.57
O I	6155.755	-3.02	-3.22	-3.63	-3.57

Table 3 continued on next page

Table 3 (*continued*)

Element	λ (Å)	$\log(X/H)_{\nu Cap}$	$\log(X/H)_{\nu Cnc}$	$\log(X/H)_{Sirius}$	$\log(X/H)_{HD72660}$
O I	6156.778	-3.02	-3.22	-3.63	-3.57
O I	6158.149	-3.02	-3.22	-3.63	-3.57
O I	6158.172	-3.02	-3.22	-3.63	-3.57
O I	6158.187	-3.02	-3.22	-3.63	-3.57
Average O I		-3.02	-3.22	-3.63	-3.57
Na I	6154.226			-5.07	-4.82
Na I	6160.747			-5.19	-4.97
Average Na I				-5.13	-4.89
Mg II	4390.572	-4.42	-4.54	-4.49	-4.42
Mg II	4427.994	-4.42	-4.52	-4.49	-4.34
Mg II	4481.126	-4.42	-4.53	-4.49	-4.38
Mg II	4481.150	-4.42	-4.53	-4.49	-4.38
Mg II	4481.325	-4.42	-4.53	-4.49	-4.38
Average Mg II		-4.42	-4.53	-4.49	-4.38
Al II	4663.056	-5.53	-5.68	-5.72	-4.90
Al I	3944.006	-5.53	-5.68	-5.72	bl.
Average Al II		-5.53	-5.68	-5.72	-4.90
Si II	4128.054	-4.28	-4.25	-4.22	-4.16
Si II	4130.894	-4.28	-4.25	-4.19	-4.16
Si II	4190.72	-4.28	-4.27	-4.15	-4.13
Si II	5041.024	-4.15	-4.15	-4.13	-4.05
Si II	5055.984	-4.32	-4.45	-4.13	-4.16
Si II	5056.317	-4.32	-4.45	-4.13	-4.16
Si II	6347.11	bl.	-4.15	-4.11	-4.05
Si II	6371.37	-4.26	-4.45	-4.11	-4.13
Average Si II		-4.27	-4.30	-4.15	-4.13
P II	6024.18	-6.55 (ul)	-6.55 (ul)	bl.	bl.
P II	6043.13	-6.55 (ul)	-6.55 (ul)	-6.55 (ul)	-6.55 (ul)
Average P II		-6.55	-6.55	-6.55	-6.55
S II	4153.06	-4.67 (ul)	-4.67	-4.44	-4.29
S II	4162.67	-4.67 (ul)	-4.67	-4.67	-4.29

Table 3 continued on next page

Table 3 (*continued*)

Element	λ (Å)	$\log(X/H)_{\nu Cap}$	$\log(X/H)_{\nu Cnc}$	$\log(X/H)_{Sirius}$	$\log(X/H)_{HD72660}$
Average S II		-4.67	-4.67	-4.55	-4.29
Ca II	3933.663	-5.74	-5.86	-6.10	-5.64
Ca II	5019.971	-5.74	-5.86	-6.10	-5.64
Average Ca II		-5.74	-5.86	-6.10	-5.64
Sc II	4246.822	-8.95	-7.68	-10.68	-10.65
Sc II	4670.407	-8.95	bl.	-10.68	-10.65
Sc II	5031.021	bl.	bl.	-10.68	-10.65
Sc II	5526.813	-8.95	-7.68	-10.68	-10.65
Average Sc II		-8.95	-7.68	-10.68	-10.65
Ti II	4163.644	-6.80	-6.03	-6.70	-6.51
Ti II	4287.873	-6.80	-5.98	-6.70	-6.51
Ti II	4290.210	-6.98	-6.28	-6.80	-6.51
Ti II	4294.090	-6.98	-6.03	-6.72	-6.51
Ti II	4300.042	-6.80	-5.93	-6.68	-6.51
Ti II	4411.072	-6.68	-5.93	-6.58	-6.51
Ti II	4468.492	-7.08	-6.07	-6.84	-6.51
Ti II	4549.622	bl.	bl.	bl.	-6.51
Ti II	4563.758	-6.98	-6.08	-6.72	-6.51
Ti II	5129.156	-6.98	-6.08	-6.75	-6.51
Ti II	5188.687	-6.98	-6.08	-6.75	-6.51
Ti II	5336.780	-6.98	-6.08	-6.75	-6.51
Average Ti II		-6.91	-6.05	-6.72	-6.51
V II	4005.71	bl.	-7.30	-7.58	-7.40
V II	4023.39	-7.40	-7.30	-7.58	-7.09
V II	4035.63	-7.40	bl.	-7.58	-7.40
V II	4036.78	-7.40	-7.30	-7.58	-7.40
Average V II		-7.4	-7.30	-7.58	-7.32
Cr II	4558.644	-6.15	-5.55	-5.71	-5.73
Cr II	4558.787	-6.15	-5.55	-5.71	-5.73
Cr II	5237.322	-6.23	-5.55	-5.75	-5.73
Cr II	5308.421	-6.15	-5.63	-5.75	na

Table 3 continued on next page

Table 3 (continued)

Element	λ (Å)	$\log(X/H)_{\nu Cap}$	$\log(X/H)_{\nu Cnc}$	$\log(X/H)_{Sirius}$	$\log(X/H)_{HD72660}$
Cr II	5313.581	-6.09	-5.55	-5.75	na
Cr II	5502.086	-6.15	-5.55	-5.75	-5.86
Average Cr II		-6.15	-5.56	-5.74	-5.76
Mn II	4206.368	-6.31	-5.76	-6.09	-6.22
Mn II	4259.19	-6.31	-5.91	-6.09	-6.22
Average Mn II		-6.31	-5.83	-6.09	-6.22
Fe II	4233.162	-4.68	-4.42	-4.10	-4.10
Fe II	4258.148	-4.68	-4.42	-4.27	-4.20
Fe II	4273.326	-4.68	-4.42	-4.27	-4.20
Fe II	4296.566	-4.68	-4.42	-4.27	-4.20
Fe II	4491.397	-4.57	-4.44	-4.32	-4.20
Fe II	4508.280	-4.72	-4.50	-4.35	-4.20
Fe II	4515.333	-4.65	-4.30	-4.32	-4.20
Fe II	4520.218	-4.65	-4.35	-4.32	-4.20
Fe II	4522.628	-4.80	-4.50	-4.39	-4.20
Fe II	4549.195	-4.68	bl.	bl.	bl.
Fe II	4549.466	-4.68	bl.	bl.	bl.
Fe II	4555.888	-4.72	-4.50	-4.35	-4.20
Fe II	4923.921	-4.68	-4.42	-4.32	-4.04
Fe II	5275.997	-4.68	-4.42	-4.32	-4.20
Fe II	5316.609	-4.68	-4.42	-4.27	-4.20
Fe II	5506.199	-4.68	-4.42	-4.20	-4.20
Average Fe II		-4.68	-4.43	-4.29	-4.18
Co II	4962.36	-7.08 (ul)	-7.08 (ul)	-7.08 (ul)	-7.08 (ul)
Co II	4964.17	-7.08 (ul)	-7.08 (ul)	-7.08 (ul)	-7.08 (ul)
Average Co II		-7.08	-7.08	-7.08	-7.08
Ni II	4679.16	-5.45	-5.15	-4.50	-5.00
Average Ni II		-5.45	-5.15	-4.50	-5.00
Sr II	4077.71	-9.03	-7.73	-8.57	-8.33
Sr II	4215.519	-9.03	-7.73	-8.73	-8.33
Average Sr II		-9.03	-7.73	-8.65	-8.33

Table 3 continued on next page

Table 3 (continued)

Element	λ (\AA)	$\log(X/H)_{\nu Cap}$	$\log(X/H)_{\nu Cnc}$	$\log(X/H)_{Sirius}$	$\log(X/H)_{HD72660}$
Y II	3982.592	-9.28	-7.16	-9.11	-8.98
Y II	5662.922	-9.28	-7.16	-9.11	-8.98
Average Y II		-9.28	-7.16	-9.11	-8.98
Zr II	3991.127	bl.	-7.40	bl.	-8.52
Zr II	3998.965	bl.	-7.40	bl.	-8.52
Zr II	4442.992	-8.70	-7.40	bl.	-8.32
Zr II	4457.431	-9.40	-7.50	bl.	bl.
Zr II	4496.962	-9.40	-7.70	-8.67	-8.40
Zr II	5112.270	-9.40	-7.32	-8.67	vw
Average Zr II		-9.22	-7.45	-8.67	-8.44
Ba II	4554.03	-9.02	-6.93	-8.50	-8.87
Ba II	4934.077	-9.02	-6.93	-8.50	-8.87
Ba II	5853.***			-8.50	-8.76
Ba II	6141.713	-9.02	-6.93	-8.46	-8.79
Average Ba II		-9.02	-6.93	-8.49	-8.82
La II	4042.91	-10.83 (ul)	-8.83	-9.49	-9.72
Average La II		-10.83	-8.83	-9.49	-9.72
Ce II	4460.21	-10.42 (ul)	-8.72	-9.34	-9.42
Average Ce II		-10.42	-8.72	-9.34	-9.42
Pr II	4222.93	-11.29 (ul.)		-9.29	-9.18
Pr III	5284.69		-9.59		
Average Pr		-11.29	-9.59	-9.29	-9.18
Nd III	5294.10	-10.50 (ul.)	-9.20	-9.10	bl.
Average Nd III		-10.5	-9.2	-9.10	
Sm II	4280.79	-10.99 (ul.)	-8.29	-8.99	-9.35
Average Sm II		-10.99	-8.29	-8.99	-9.35
Eu II	4129.70		-9.61	-10.64	-10.79
Average Eu II			-9.61	-10.64	-10.79
Gd II	4037.32	-10.88 (ul.)	-8.18	-9.58	-9.48
Average Gd II		-10.88	-8.18	-9.58	-9.48

Table 3 continued on next page

Table 3 (continued)

Element	λ (\AA)	$\log(X/H)_{\nu Cap}$	$\log(X/H)_{\nu Cnc}$	$\log(X/H)_{Sirius}$	$\log(X/H)_{HD72660}$
Tb II	4005.47	bl.	bl.	bl.	bl.
Tb II	4033.027	bl.	bl.	bl.	bl.
Dy II	4000.45	-10.86 (ul.)	bl.	-9.38	-9.68
Dy II	4077.97	bl.	bl.	bl.	-9.68
Average Dy II		-10.86		-9.38	-9.68
Ho II	4045.45	bl.	bl.	bl.	-9.74
Ho II	4152.62	-11.74 (ul.)	bl.	-10.26	-9.48
Average Ho II		-11.74		-10.26	-9.61
Er II	4142.91	bl.	-8.17	-9.59	-9.99
Average Er II			-8.17	-9.59	-9.99
Tm II	4242.15	bl.	bl.	bl.	-10.0
Average Tm II					-10.0
Yb II	4135.095	-10.92 (ul.)	-7.44	-10.92 (ul.)	-8.62
Average Yb II		-10.92	-7.44	-10.92	-8.62
Hf II	4417.36	bl.	bl.	bl.	bl.
Hf II	3918.08				-9.42
Average Hf II					-9.42
Os II	4158.44	-10.55	-6.85	-10.55	-7.55
Average Os II		-10.55	-6.85	-10.55	-7.55
Pt II	4514.17	-10.20 (ul.)	-7.20	-8.17	bl.
Average Pt II		-10.20	-7.20	-8.17	
Hg II	3983.931	-10.91 (ul.)	-7.82	-9.71	-9.20
Average Hg II		-10.91	-7.82	-9.71	-9.20

Table 4. Abundance uncertainties for the elements analysed in HR 8844

		HeI	CII	OI	MgII	AlII	SiII	SII	CaII
ΔT_{eff}	+200 K	-0.30	0.00	0.05	0.047	0.075	-0.017	0.00	0.109
$\Delta \log g$	0.15 dex	0.079	0.24	-0.06	-0.052	0.118	-0.017	-0.12	-0/032
$\Delta \xi_t$	+0.20 km s ⁻¹	0.00	0.00	0.00	0.00	0.075	-0.035	-0.046	0.00
$\Delta \log gf$	+0.10	-0.30	-0.12	-0.16	-0.25	-0.028	-0.053	-0.071	-0.105
$\Delta_{\text{continuum}}$		-0.12	0.21	0.075	0.13	0.25	0.062	0.061	0.058
$\sigma_{[X/H]}$		0.45	0.34	0.19	0.29	0.20	0.092	0.159	0.165
		ScII	TiII	VII	CrII	MnII	FeII	NiII	SrII
ΔT_{eff}	+200 K	0.22	0.041	0.028	0.057	0.00	0.079	0.176	0.138
$\Delta \log g$	0.15 dex	-0.079	0.015	-0.014	0.03	0.007	0.041	0.114	-0.058
$\Delta \xi_t$	+0.20 km s ⁻¹	-0.038	-0.016	0.00	0.00	0.00	-0.095	0.00	-0.058
$\Delta \log gf$	+0.10	-0.13	-0.23	-0.046	-0.15	-0.015	-0.095	-0.155	-0.058
$\Delta_{\text{continuum}}$		0.067	0.03	0.014	0.046	0.014	0.0126	0.079	0.051
$\sigma_{[X/H]}$		0.276	0.064	0.23	0.169	0.076	0.162	0.273	0.178
		YII	ZrII	BaII	LaII	CeII	PrII	NdII	SmII
ΔT_{eff}	+200 K	0.146	0.058	0.114	0.11	0.11	0.11	0.11	0.11
$\Delta \log g$	0.15 dex		0.046	-0.032	-0.125	-0.13	-0.13	-0.13	-0.13
$\Delta \xi_t$	+0.20 km s ⁻¹	0.00	0.00	-0.097	-0.09	-0.09	-0.09	-0.09	-0.09
$\Delta \log gf$	+0.10	-0.05	-0.066	-0.125	-0.13	-0.13	-0.13	-0.13	-0.13
$\Delta_{\text{continuum}}$		0.041	0.146	-0.097	-0.09	-0.09	-0.09	-0.09	-0.09
$\sigma_{[X/H]}$		0.165	0.173	0.251	0.25	0.25	0.25	0.25	0.25
		EuII	GdII	DyII	TbII	HoII	ErII	HgII	
ΔT_{eff}	+200 K	0.11	0.11	0.11	0.11	0.11	0.11	-0.155	
$\Delta \log g$	0.15 dex	-0.13	-0.13	-0.13	-0.13	-0.13	-0.13	0.041	
$\Delta \xi_t$	+0.20 km s ⁻¹	-0.09	-0.09	-0.09	-0.09	-0.09	-0.09	-0.097	
$\Delta \log gf$	+0.10	-0.13	-0.13	-0.13	-0.13	-0.13	-0.13	-0.108	
$\Delta_{\text{continuum}}$		-0.09	-0.09	-0.09	-0.09	-0.09	-0.09	0.079	
$\sigma_{[X/H]}$		0.25	0.25	0.25	0.25	0.25	0.25	0.23	

Table 5. Bibliographical references for the atomic data.

Element	Bibliographical source
He I	Ma60= Martin (1960)
He I	DR2006= Drake (2006)
C II	NIST/ASD= Kramida et al. (2017)
O I	KZ91= Butler, K. & Zeippen, C. J. (1991)
O I	W96= Wiese et al. (1996)
O I	NIST/ASD= Kramida et al. (2017)

Table 5 continued on next page

Table 5 (continued)

Element	Bibliographical source
Mg II	NIST/ASD= Kramida et al. (2017)
Mg II	NIST/ASD= Kramida et al. (2017)
Al II	NIST/ASD= Kramida et al. (2017)
Al I	NIST/ASD= Kramida et al. (2017)
Si II	NIST/ASD= Kramida et al. (2017)
Si II	Sh61= Shenstone (1961)
S II	GUES= Kurucz (1993)
S II	KP= Kurucz & Peytremann (1975)
S II	MWRB= Miller et al. (1974)
Ca II	NIST="http://physics.nist.gov/PhysRefData/ASD/"
Ca II	T89= Theodosiou (1989)
Sc II	NIST/ASD= Kramida et al. (2017)
Ti II	NIST/ASD= Kramida et al. (2017)
Ti II	NIST/ASD= Kramida et al. (2017)
Ti II	NIST/ASD= Kramida et al. (2017)
Ti II	NIST/ASD= Kramida et al. (2017)
V II	K10= Kurucz (2010)
V II	BGF= Biemont et al. (1989)
V II	WLDSC= Wood et al. (2014)
Cr II	SN14= Sansonetti & Nave (2014)
Mn II	KL01= Kling et al. (2001)
Fe II	NIST/ASD= Kramida et al. (2017)
Fe II	RU98= Raassen & Uylings (1998)
Ni II	K03= Kurucz (2003)
Sr II	PBL95= Pinnington et al. (1995)
Y II	Bie11= Biémont et al. (2011)
Y II	MCS75= Meggers et al. (1975a)
Zr II	L06= Ljung et al. (2006)
Ba II	NBS= Miles & Wiese (1969)
Ba II	DSVD92= Davidson et al. (1992)
La II	Zi99= Zhiguo et al. (1999)
Ce II	LSCI= Lawler et al. (2009)

Table 5 continued on next page

Table 5 (*continued*)

Element	Bibliographical source
Ce II	PQWB= Palmeri et al. (2000)
Pr III	ISAN= Ryabtsev (2010)
Nd III	RRKB= Ryabchikova et al. (2006)
Sm II	LA06= Lawler et al. (2006)
Eu II	LWHS= Lawler et al. (2001b)
Eu II	ZLLZ= Zhiguo et al. (2000)
Gd II	DH06= Den Hartog et al. (2006)
Dy II	WLN= Wickliffe et al. (2000)
Dy II	MC= Meggers et al. (1975b)
Gd II	DH06= Den Hartog et al. (2006)
Tb II	LA01= Lawler et al. (2001a)
Ho II	LA04= Lawler et al. (2004)
Er II	LA08= Lawler et al. (2008)
Hg II	SR01= Sansonetti & Reader (2001)
Hg II	Do03= Dolk et al. (2003)

Table 6. Comparison of the derived abundances for HR 8844 derived in this work with the ones of [Royer et al. \(2014\)](#).

Element	$\log(X/H)_{HR8844}$ this work	$\log(X/H)_{HR8844}$ (Royer et al. 2014)
C	-3.880	-3.700
O	-3.270	-3.300
Mg	-4.770	-4.280
Si	-4.510	-4.208
Ca	-5.830	-5.823
Sc	-8.990	-9.223
Ti	-6.830	-7.015
Cr	-6.180	-6.098
Fe	-4.500	-4.466
Sr	-8.330	-8.480
Y	-8.460	-9.500
Zr	-8.630	-8.900

Table 7. Comparison of the derived abundances for ν Cap, ν Cnc, Sirius A and HD 72660 with previous analyses. A91 refers to Adelman (1991), SD93 to Smith & Dworetzky (1993), A89 to Adelman (1989), L11 to Landstreet (2011), C16 to Cowley et al. (2016) and GL16 to Golriz & Landstreet (2016).

Element	$\log(X/H)_{\nu Cap}$	A91 and SD93	$\log(X/H)_{\nu Cnc}$	A89	$\log(X/H)_{Sirius}$	L11 and C16	$\log(X/H)_{HD72660}$	GL16
He	-1.07	-1.19	-1.47	-1.57	-1.77	-1.24		
C	-3.48	-3.69 , -3.39	-3.78	-3.88	-4.04	-4.55	-4.15	-4.10
N	-4.02	-4.26			-4.02	-4.08	-4.02	-4.70
O	-3.02	-3.33			-3.63	-3.60	-3.57	-2.50
Na					-5.13	-4.7		
Mg	-4.42	-4.61	-4.53	-4.71	-4.49	-4.70	-4.38	-4.20
Al	-5.53	-6.03	-5.68	-6.38	-5.72	-5.65	-4.90	-4.90
Si	-4.27	-4.69	-4.30	-4.59	-4.15	-4.40	-4.13	-4.20
P					-6.55	-6.70	-6.55	-7.10
S	-4.67	-4.85	-4.67	-5.05	-4.55	-4.80	-4.29	-4.50
Ca	-5.74	-5.55	-5.86	-6.06	-6.10	-6.00	-5.64	-5.40
Sc	-8.95	-9.34	-7.68	-8.19	-10.68	-10.03	-10.65	-9.50
Ti	-6.91	-7.05	-6.05	-6.38	-6.72	-6.90	-6.51	-6.60
V	-7.40	-7.64	-7.30	-8.20	-7.58	-7.27	-7.32	-7.20
Cr	-6.15	-6.4; -6.13	-5.56	-5.88	-5.74	-5.75	-5.76	-5.65
Mn	-6.31	-6.80; -6.69	-5.83	-5.88	-6.09	-6.05	-6.22	-5.90
Fe	-4.68	-4.60; -4.47	-4.43	-4.60	-4.29	-4.20	-4.18	-3.75
Co	-7.08	-6.7	-7.08	-6.23	-7.08	-6.6	-7.08	-6.50
Ni	-5.45	-5.80; -5.67	-5.15	-5.62	-4.50	-5.15	-5.00	-5.15
Sr	-9.03	-8.77	-7.73	-8.01	-8.65	-8.57		
Y			-7.16	-7.76	-9.11	-9.14	-8.98	-7.90
Zr	-9.22	-9.36	-7.45	-7.60	-8.67	-8.75	-8.44	-8.30
Ba	-9.02	-9.29	-6.93	-6.97	-8.49	-8.40; -8.47	-8.82	-9.65
La					-9.49	-9.33		
Ce					-9.34	-8.92		
Pr					-9.29	-9.09		
Nd					-9.10	-9.10		
Sm					-8.99	8.99		
Eu					-10.64	-10.19		
Gd			-8.18	-9.29	-9.58	-9.28		
Dy					-9.38	-9.16		
Ho					-10.26	-9.94		
Er					-9.59	-9.27		
Yb					-10.92	-9.12	-8.62	-9.00
Os					-10.55	-9.55	-7.55	-12
Pt					-8.17	-8.60		
Hg			-7.82	-7.82	-9.71	-9.71	-9.20	-9.20

ALL AUTHORS AND AFFILIATIONS

R. MONIER¹,

LESIA, UMR 8109, Observatoire de Paris et Université Pierre et Marie Curie Sorbonne Universités, place J. Janssen, Meudon.

M. GEBRAN²,

Department of Physics and Astronomy, Notre Dame University-Louaize, PO Box 72, Zouk Mikael, Lebanon.

F. ROYER³,

GEPI, Observatoire de Paris, place J. Janssen, Meudon, France.

T. KILICOGU⁴,

Department of Astronomy and Space Sciences, Faculty of Science, Ankara University, 06100, Turkey.

AND

Y. FRÉMAT⁵.

Royal observatory of Belgium, Dept. Astronomy and Astrophysics, Brussels, 8510, Belgium.